

MIT Open Access Articles

Bulk Universality for Random Lozenge Tilings Near Straight Boundaries and for Tensor Products

The MIT Faculty has made this article openly available. **Please share** how this access benefits you. Your story matters.

Citation: Gorin, V. "Bulk Universality for Random Lozenge Tilings near Straight Boundaries and for Tensor Products." *Communications in Mathematical Physics* (2016): 1-28.

As Published: 10.1007/S00220-016-2801-X

Publisher: Springer Nature

Persistent URL: <https://hdl.handle.net/1721.1/134457>

Version: Author's final manuscript: final author's manuscript post peer review, without publisher's formatting or copy editing

Terms of use: Creative Commons Attribution-Noncommercial-Share Alike



BULK UNIVERSALITY FOR RANDOM LOZENGE TILINGS NEAR STRAIGHT BOUNDARIES AND FOR TENSOR PRODUCTS

VADIM GORIN

ABSTRACT. We prove that the asymptotic of the bulk local statistics in models of random lozenge tilings is universal in the vicinity of straight boundaries of the tiled domains. The result applies to uniformly random lozenge tilings of large polygonal domains on triangular lattice and to the probability measures describing the decomposition in Gelfand–Tsetlin bases of tensor products of representations of unitary groups. In a weaker form our theorem also applies to random domino tilings.

1. INTRODUCTION

1.1. Overview. This article is about random *lozenge tilings*, which are tilings of domains on the regular triangular grid by rhombuses of three types (see Figures 1, 2, 3, 4, 5), and which can be identified with dimers, discrete stepped surfaces, $3d$ Young diagrams, see e.g. [K2], [BP, Section 2]. In more details, we are interested in the asymptotic behavior of *Gibbs measures* on tilings, which means that tilings in each subdomain are always conditionally uniformly distributed given boundary conditions, i.e. positions of lozenges surrounding this domain. There are several ways to produce such Gibbs measures. From the point of view of statistical mechanics, the most natural one is to fix a very large planar domain and consider the uniform measure on *all* (finitely many) lozenge tilings of this domain. Asymptotic representation theory suggests two more ways, related to decompositions of tensor products of representations of classical Lie groups and restrictions of characters of the infinite-dimensional counterparts of these groups, see e.g. [BuG1], [BBO]. Finally, one can also *grow* tilings by means of interacting particle systems, see e.g. [BG], [BF].

The rigorous asymptotic results available in the literature for various random lozenge tilings models all share the same features. Let us describe such features on the example of the uniformly random lozenge tilings of an $A \times B \times C$ hexagon as $A, B, C \rightarrow \infty$ (in such a way that A/B and A/C converge to constants), see Figure 1. Note that such tilings can be linked both to decompositions of certain irreducible representations (cf. [BP]) and to growth models (see [BG]).

The following asymptotic features of the tilings of hexagons are known:

- The random lozenge tilings exhibit the *law of large numbers*, cf. Section 3. One way to phrase it is that in each macroscopic sub-region of the hexagon the asymptotic proportions of three types of lozenges converge in probability to deterministic numbers, described by integrals over this sub-domain of three functions $p^{\blacktriangledown}(\cdot)$, $p^{\blacktriangleright}(\cdot)$, and $p^{\blacktriangleleft}(\cdot)$. In particular, outside the inscribed ellipse one observes the *frozen region* where asymptotically only one type of lozenges remains present, see [CLP], [CKP], [BuG1]. The region where all three types of lozenges are asymptotically present is called *liquid*.
- The global fluctuations of the *height function* of tiling (see Section 3 for the detailed definition) are asymptotically normal and can be described via the

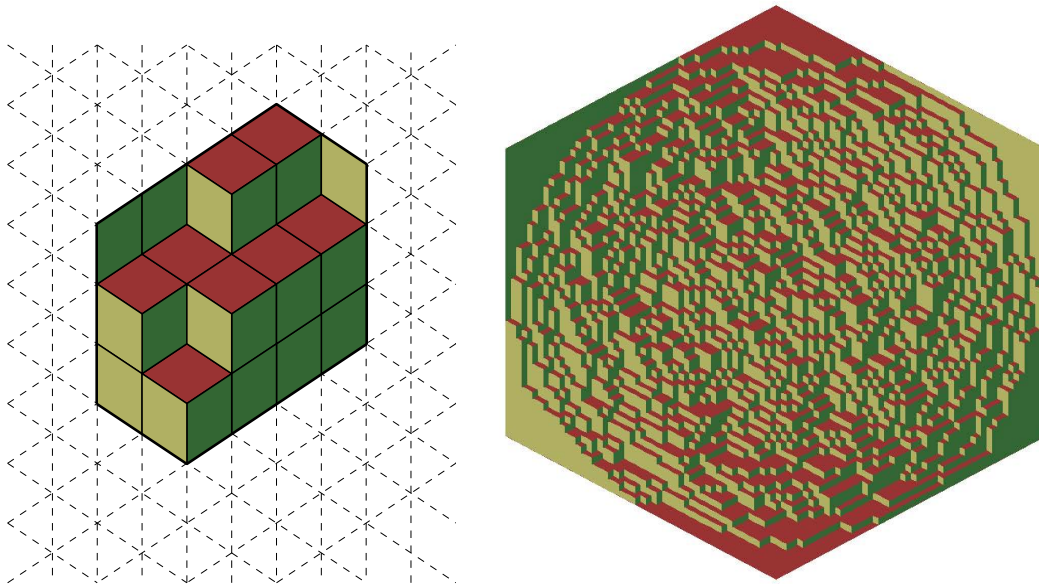


FIGURE 1. Uniformly random lozenge tilings of $3 \times 4 \times 2$ and $50 \times 50 \times 50$ hexagons.

pullback of the Gaussian Free Field with Dirichlet boundary conditions, see [Pe2], [D], [BuG2].

- Locally, near each point inside the inscribed ellipse in the limit one observes a *translation invariant ergodic Gibbs measure* on lozenge tilings of the plane. Its *slope* is determined by the law of large numbers (such measure is unique for each slope, see [She], and its correlation functions admit known closed expressions, cf. Section 4), see [BKMM], [G], [Pe1].
- The one-point fluctuations of the boundary of the frozen region at generic point after proper rescaling converge to the Tracy–Widom distribution F_{GUE} , and multi-point fluctuations are described by the Airy line ensemble, see [BKMM], [Pe1].¹
- At a point where the frozen boundary is tangent to a side of the hexagon, the fluctuations are described by the GUE–corners process, see [JN], [Nor], [GPa], [Nov].

The *universality belief* predicts that all these features should be very robust along different models of lozenge tilings, and should not depend on details. It means, that while the limit shape (i.e. the asymptotic proportions $p^{\square}(\cdot)$, $p^{\triangleleft}(\cdot)$, $p^{\triangleright}(\cdot)$) and the exact shape of the boundaries of the frozen regions differ from system to system, but they should always exist. The fluctuations of the height function should always be given by a pullback of the Gaussian Free Field, and only the map with respect to which this pullback is taken, might change. Bulk local limits should be always described by translation invariant Gibbs measures and only the slope of such measure might vary from system to system. Finally, the fluctuations of the boundaries of frozen regions should be always governed by the Tracy–Widom distribution, Airy line ensemble and GUE–corners process.

¹For tilings of more complicated regions, the boundary of the frozen region might develop various singularities, which lead to different behaviors.

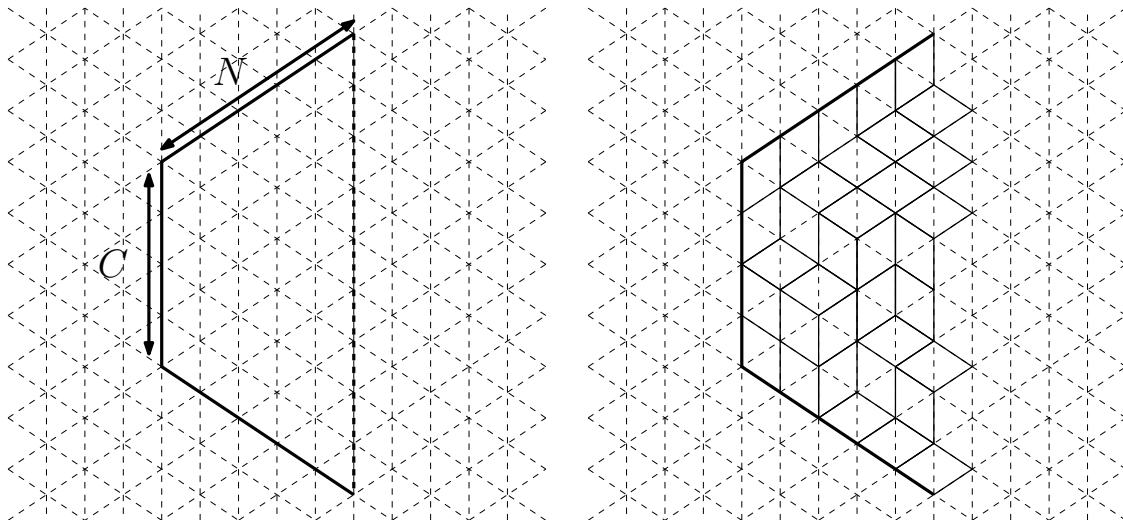


FIGURE 2. Trapezoid $\Omega_{N,C}$ with $N = 5$, $C = 4$ and one of its tilings.

While this conjectural universality is confirmed by numerous examples, but by now only the Law of Large Numbers has been proven in sufficient generality, cf. [CKP], [KO], [BuG1].

In the present article we address the third feature about local (also called “bulk”) scaling limits. In simple words, we show that whenever for a random lozenge tiling the law of large numbers holds, if the tiled domain has a straight boundary, then near this boundary the *universality* for the local limits is valid.

1.2. Results. We proceed to a more detailed formulation of our main result.

Consider a trapezoid drawn on the triangular grid as shown in Figure 2. Such domain is parameterized by the length of the left vertical side C and the width N and we denote it $\Omega_{N,C}$. Consider the set of all tilings of $\Omega_{N,C}$, in which we allow horizontal lozenges to *stick out* of the right boundary. The combinatorial constraints imply that there are precisely N horizontal lozenges sticking out. Let \mathcal{P} be a probability measure on tilings of $\Omega_{N,C}$ which satisfies the *Gibbs property*, which means that given the positions of the N horizontal lozenges on the boundary the conditional distribution of the tilings becomes uniform.

Further, given a tiling ω of $\Omega_{N,C}$ with coordinates of the sticking out horizontal lozenges $\ell_1 > \ell_2 > \dots > \ell_N$, let

$$\mu(\omega) = \frac{1}{N} \sum_{i=1}^N \delta_{\ell_i/N}$$

be a probability measure encoding them. Then the pushforward of \mathcal{P} with respect to the map $\omega \mapsto \mu(\omega)$ is a *random* probability measure $\mu_{\mathcal{P}}$. Due to the Gibbs property, \mathcal{P} is uniquely reconstructed by $\mu_{\mathcal{P}}$.

Note that each tiling of $\Omega_{N,C}$ can be viewed also as a tiling of $\Omega_{N,C+1}$, by adding a row of ∇ lozenges on top. For example, the tiling $\Omega_{5,4}$ in the right panel of Figure 2 is simultaneously a tiling of $\Omega_{5,3}$ with added row on top. Because of this correspondence, if we fix the coordinates of horizontal lozenges along the right boundary, then the exact value of C in $\Omega_{N,C}$ becomes not important (as long as it is large enough). In the same

way, in order to reconstruct a \mathcal{P} -random tiling by $\mu_{\mathcal{P}}$ we actually do not need to know the value of C .

Theorem 1.1. *Let $\Omega_{N,C(N)}$, $N = 1, 2, \dots$, be a sequence of trapezoids equipped with probability measures $\mathcal{P}(N)$ on their lozenge tilings. Suppose that:*

- (A) $\frac{C(N)}{N}$ stays bounded as $N \rightarrow \infty$.
- (B) The random probability measures $\mu_{\mathcal{P}(N)}$ converge (weakly, in probability) to a deterministic probability measure μ .

Then

- (1) The $\mathcal{P}(N)$ -random lozenge tilings of $\Omega_{N,C(N)}$ exhibit the Law of Large Numbers as $N \rightarrow \infty$: there are three deterministic densities $p^{\square}(\mathbf{x}, \boldsymbol{\eta})$, $p^{\lozenge}(\mathbf{x}, \boldsymbol{\eta})$, and $p^{\diamond}(\mathbf{x}, \boldsymbol{\eta})$, $0 < \boldsymbol{\eta} < 1$, $\mathbf{x} \in \mathbb{R}$, such that for any subdomain $\mathcal{D} \subset \frac{1}{N}\Omega_{N,C(N)}$ with smooth boundary, the normalized by N (random) numbers of lozenges of types $(\square, \lozenge, \diamond)$ inside $N\mathcal{D}$ converge in probability to the vector

$$\left(\int_{\mathcal{D}} p^{\square}(\mathbf{x}, \boldsymbol{\eta}) d\mathbf{x}d\boldsymbol{\eta}, \int_{\mathcal{D}} p^{\lozenge}(\mathbf{x}, \boldsymbol{\eta}) d\mathbf{x}d\boldsymbol{\eta}, \int_{\mathcal{D}} p^{\diamond}(\mathbf{x}, \boldsymbol{\eta}) d\mathbf{x}d\boldsymbol{\eta} \right)$$

- (2) Take a point $(\mathbf{x}, \boldsymbol{\eta})$, such that all three asymptotic densities at this point are continuous and non-zero. Assume $0 < \boldsymbol{\eta} < 1$. If $n(N)$, $x(N)$ are two sequences of integers, such that $\lim_{N \rightarrow \infty} n(N)/N = \boldsymbol{\eta}$, $\lim_{N \rightarrow \infty} x(N)/N = \mathbf{x}$, then the point process of lozenges near the point $(n(N), x(N))$ weakly converges as $N \rightarrow \infty$ to the (unique) translation invariant ergodic Gibbs measure on lozenge tilings of slope $(p^{\square}(\mathbf{x}, \boldsymbol{\eta}), p^{\lozenge}(\mathbf{x}, \boldsymbol{\eta}), p^{\diamond}(\mathbf{x}, \boldsymbol{\eta}))$.

A more detailed formulation and the proof is below in Theorems 4.1, 4.3. Of course, for the domains obtained from $\Omega_{N,C}$ by rotating it by $60 \cdot k$ degrees, $k = 1, 2, 3, 4, 5$, the exact analogue of Theorem 1.1 is also valid.

The conditions (A) and (B) of Theorem 1.1 are known to hold for many models of lozenge tilings, which implies that the local convergence to the translation invariant Gibbs measures is true for them. Let us provide some examples:

Corollary 1.2. *Let Ω be any simply-connected polygonal domain on the triangular grid, and define $\Omega(L)$, $L = 1, 2, \dots$ to be the domain obtained by multiplying all the side lengths of Ω by L . For any part of $\Omega(L)$ covered by a trapezoid, near any point in the liquid region in this part, the uniformly random lozenge tilings of $\Omega(L)$ converge locally to the ergodic translation-invariant Gibbs measure of the corresponding slope.*

Let us elaborate on the notion of a part of $\Omega(L)$ covered by a trapezoid. Of course, one can always consider a huge trapezoid, such that the the entire domain $\Omega(L)$ will be inside. However, that's not what we want. We rather require the part to be such that the restrictions of the uniformly random tilings of the entire domain to this part are described by Gibbs probability measures on tilings of the trapezoid in the context of Theorem 1.1. In particular, three sides of such trapezoid should belong to the same lines as sides of $\Omega(L)$, cf. Figure 3. Section 4 explains this notion in more details and culminates in Theorem 4.5 which is a refinement of Corollary 1.2.

Remark 1.3. Many polygonal domains can be *completely covered* by trapezoids, which implies the convergence to the ergodic translation-invariant Gibbs measures *everywhere* in the liquid region, cf. Figure 3 for examples. Yet more complicated domains are covered only partially, cf. Figure 4.

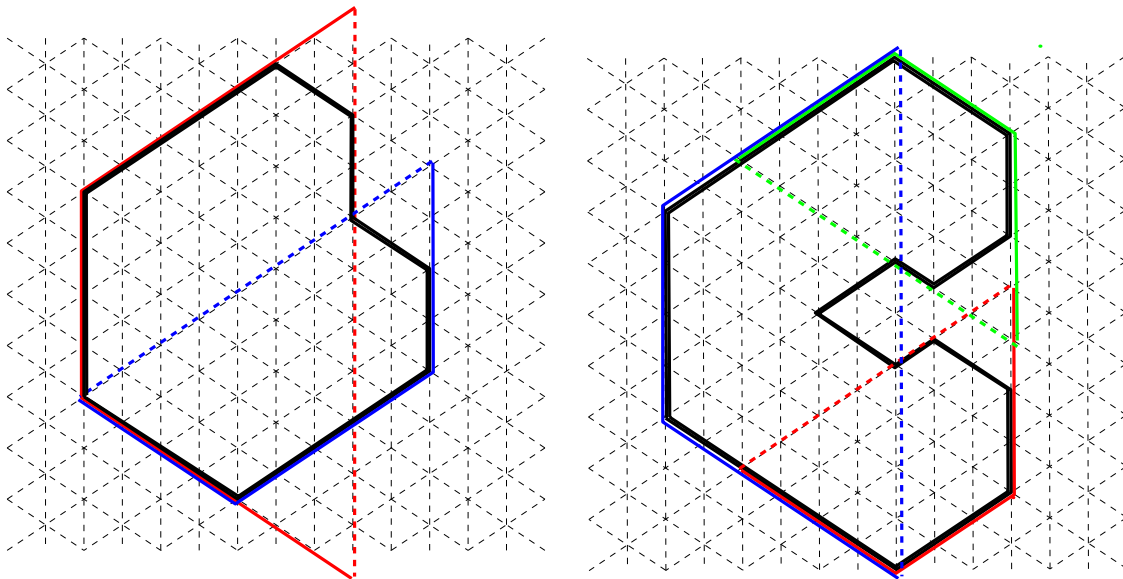


FIGURE 3. Left panel: the heart-shaped polygon (in black) is covered by two trapezoids. Right panel: the C-shaped polygon (in black) is covered by three trapezoids.

Remark 1.4. For specific polygons, which are covered by a *single* trapezoid, an analogue of Corollary 1.2 was previously proven in [Pe1]. For a class of (non-polygonal) domains, such that the limit shape has *no frozen regions* an analogue of Corollary 1.2 was previously proven in [K1]. A general conjecture that the bulk asymptotic behavior of Corollary 1.2 should hold *universally* for tilings of finite planar domains dates back to [CKP].

Remark 1.5. The tiled domains do not have to be polygonal, see Theorem 4.5 for the detailed formulation. The assumption of being simply-connected is also probably not essential, however, most Law of Large Numbers type theorems in the literature stick to this assumption for simplicity, and so we have to use it here as well. There are examples of domains with holes for which the Law of Large Numbers is explicitly known (see e.g. [BGG, Section 9.2]), and for them Corollary 1.2 holds.

Another example comes from the representation theory. Recall that the irreducible representations of the N -dimensional unitary group $U(N)$ are parameterized by N -tuples of integers $\lambda_1 \geq \lambda_2 \geq \dots \geq \lambda_N$ called *signatures*, see e.g. [W]. It is convenient to shift the coordinates by introducing strictly ordered coordinates $\ell_i = \lambda_i - i$, $i = 1, \dots, N$. We denote the corresponding irreducible representation through T_ℓ . Such representation has a distinguished *Gelfand–Tsetlin basis*, parameterized by the *Gelfand–Tsetlin patterns*, which are in bijection with lozenge tilings of trapezoidal domains as above. Here the coordinates of the horizontal lozenges sticking out of the right boundary of the domain are precisely the label $\ell_1 > \ell_2 > \dots > \ell_N$ of the representation, see [BP] and also Section 2 for the details. In particular, the dimension $\dim(T_\ell)$ equals the total number of the tilings of trapezoidal domain with fixed N lozenges along the right boundary.

If we take any *reducible* (finite-dimensional) representation T of $U(N)$, then we can decompose it into irreducible components $T = \oplus_\ell c_\ell T_\ell$ and further consider the Gelfand–Tsetlin basis in each of them. Recalling the bijection with tilings, we thus determine for each lozenge tiling of trapezoidal domain a non-negative number, which

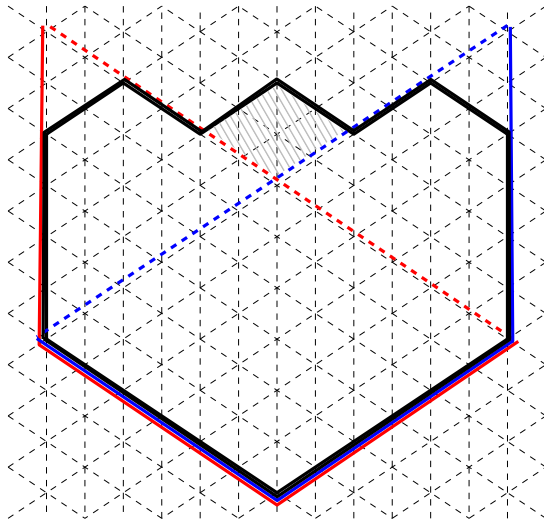


FIGURE 4. Most of this domain is covered by two trapezoids, yet we can not cover the shaded gray region. Therefore, Corollary 1.2 applies everywhere except the gray region.

is equal to c_ℓ with ℓ encoding the horizontal lozenges along the right vertical boundary of the domain. All these numbers sum up to $\dim(T)$, so that after dividing by $\dim(T)$ they define a probability measure \mathcal{P}^T on lozenge tilings. Varying T in this construction one arrives at several intriguing probability distributions.

The first example is given by the tensor product of two irreducible representations.

Corollary 1.6. *Let $\ell(N), \kappa(N)$ be two sequences of signatures (in the notation with strictly increasing coordinates) such that*

- *The numbers $\frac{\ell_i(N)}{N}, \frac{\kappa_i(N)}{N}, 1 \leq i \leq N$ are uniformly bounded.*
- *There exist two monotonous functions f^ℓ, f^κ with finitely many points of discontinuity and such that*

$$\lim_{N \rightarrow \infty} \frac{1}{N} \sum_{i=1}^N \left| f^\ell \left(\frac{i}{N} \right) - \frac{\ell_i(N)}{N} \right| = \lim_{N \rightarrow \infty} \frac{1}{N} \sum_{i=1}^N \left| f^\kappa \left(\frac{i}{N} \right) - \frac{\kappa_i(N)}{N} \right|.$$

Consider the tensor product $T(N) = T_{\ell(N)} \otimes T_{\kappa(N)}$ and the corresponding measure on lozenge tilings $\mathcal{P}^{T(N)}$. Then the conclusion of Theorem 1.1 is valid for $\mathcal{P}^{T(N)}$ as $N \rightarrow \infty$.

The proof of Corollary 1.6 is a combination of Theorem 1.1 with [BuG1, Theorem 1.1] describing the Law of Large Numbers for the tensor products.

We remark that since Theorem 1.1 is restricted to $0 < \eta < 1$, we do not get any information about $\eta = 1$, i.e. the behavior of the lozenges at the right boundary of the domain. *Conjecturally* this behavior should be similar, cf. [BES] for the recent results in this direction for sums of random matrices, which are continuous analogues of tensor products (see e.g. [BuG1, Section 1.3]).

Another celebrated representation of $U(N)$ is $(\mathbb{C}^N)^{\otimes n}$, which was intensively studied in the context of the *Schur–Weyl duality*, cf. [W].

Corollary 1.7. *Consider the representation of $U(N)$ in $(\mathbb{C}^N)^{\otimes n}$ by natural action in each component of the tensor product. Suppose that as $N \rightarrow \infty$, n varies in such a way that $\lim_{N \rightarrow \infty} n/N^2 = c > 0$. Let \mathcal{P}^N denote the probability measure on lozenge*

tilings corresponding to the decomposition of this representation. Then the conclusion of Theorem 1.1 is valid for \mathcal{P}^N as $N \rightarrow \infty$.

The proof of Corollary 1.7 is a combination of Theorem 1.1 with the Law of Large Numbers for the decomposition of $(\mathbb{C}^N)^{\otimes n}$ obtained in [Bi], see also [BuG1, Theorem 5.1]

Corollaries 1.2, 1.6, 1.7 do not exhaust the list of possible applications of Theorem 1.1 and we refer e.g. to [BBO], [Pa1], [Pa2] for some further examples of the situations where this theorem holds. Further, Theorem 1.1 also has consequences for *domino* tilings on square grid, as in [BuK]. In more details, it implies that in the particle process corresponding to the rectangular parts of domains tiled with dominos, the 1d bulk scaling limit along a section is universally governed by the discrete Sine process, see Section 4 for the definition of the discrete Sine process and [BuK, Appendix B] for the exact statement.

1.3. Discussion. One way to interpret Theorem 1.1 is that straight boundaries lead to a *smoothing effect*. Indeed, we do not know much about the local structure of random measures $\mu_{\mathcal{P}(N)}$, and it can be anything, yet as soon as we move macroscopic distance towards the straight boundary, the local measures become universal. This interpretation can be put into a wider context by observing that the stochastic process of $N-t$ horizontal lozenges on $(N-t)$ th (from the right) vertical line of a trapezoid $\Omega_{N,C}$ is a Markov chain in time variable t , as follows from the Gibbs property. Therefore, we see that this Markov chain has a *homogenization* property, i.e. its local statistics become universal. In a parallel work [GPe] we study a similar homogenization for the families of non-intersecting paths on very short time scales.

In the continuous setting there is a close analogy with the homogenization properties of *Dyson Brownian Motion*. Such property was first observed in [J], and used there for proving the universality of the local statistics for certain ensembles of Wigner random matrices. More recently, such homogenization was developed much further and has led to many exciting universality results, see e.g. [Shc], [BEY], [LY] and references therein.

It is natural to ask whether an analogue of Theorem 1.1 can hold for other conjectural universal features of the lozenge tilings, such as the fluctuations of the frozen boundary or global fluctuations of the height function. Regrettably, the answer is *no*, the knowledge of the Law of Large Numbers at the right boundary of the trapezoid domain is not enough for proving other universal features. A simple way to see that is to take a Bernoulli random variable ζ and to add $\lfloor \zeta \sqrt{N} \rfloor$ to the coordinates of the lozenges at the right boundary. This addition clearly does not change the Law of Large Numbers (the assumption of Theorem 1.1), yet it will lead to the same shift everywhere in the tiling, and therefore will influence all the conjectural limiting behaviors, *except* for the local bulk limits that we study here. We also refer to [DJM, Section 1.9] for a related discussion.

1.4. Our methods. The proof of Theorem 1.1 is based on several ingredients. The first one is the double contour integral expression of [Pe1] for the correlation kernel of the determinantal point process describing the uniformly random lozenge tilings of trapezoids with *fixed* positions of horizontal lozenges on the right boundary. Our asymptotic analysis of this kernel reveals a new fact: the bulk asymptotic behavior depends only on the global scale law of large numbers for the right boundary. This paves a way to pass from fixed to random horizontal lozenges on the right boundary.

Let us emphasize that in the latter random boundary case the correlation functions of the point process of lozenges inside the domain do not have to be determinantal (and we do not expect any explicit formulas for them); yet, this turns out to be irrelevant for our asymptotic analysis.

We also need to make a link between the slope of the local limiting Gibbs measure and the slope in the global Law of Large Numbers, for which we make use of the description of [BuG1] of the limit shape through the quantization of the Voiculescu R -transform.

1.5. Acknowledgements. The author would like to thank Alexei Borodin, Alexey Bufetov and Leonid Petrov for helpful discussion. This work was partially supported by the NSF grant DMS-1407562 and by the Sloan Research Fellowship.

2. GELFAND–TSETLIN PATTERNS WITH FIXED TOP ROW

For a fixed $N = 1, 2, \dots$ let $\mathbf{t} = (\mathbf{t}_1 > \mathbf{t}_2 > \dots > \mathbf{t}_N)$ be an N tuple of integers. A *Gelfand–Tsetlin pattern* with top row \mathbf{t} is an array of $N(N + 1)/2$ integers x_i^j , $1 \leq i \leq j \leq N$, which satisfy the interlacing condition

$$x_j^{i+1} \geq x_j^i > x_{j+1}^i, \quad 1 \leq i \leq j \leq N - 1,$$

and the top row condition $x_i^N = \mathbf{t}_i$, $i = 1, \dots, N$. Such patterns are in bijection with lozenge tilings of certain specific domains, shown in Figure 5; the bijection is given by positions of horizontal lozenges.²

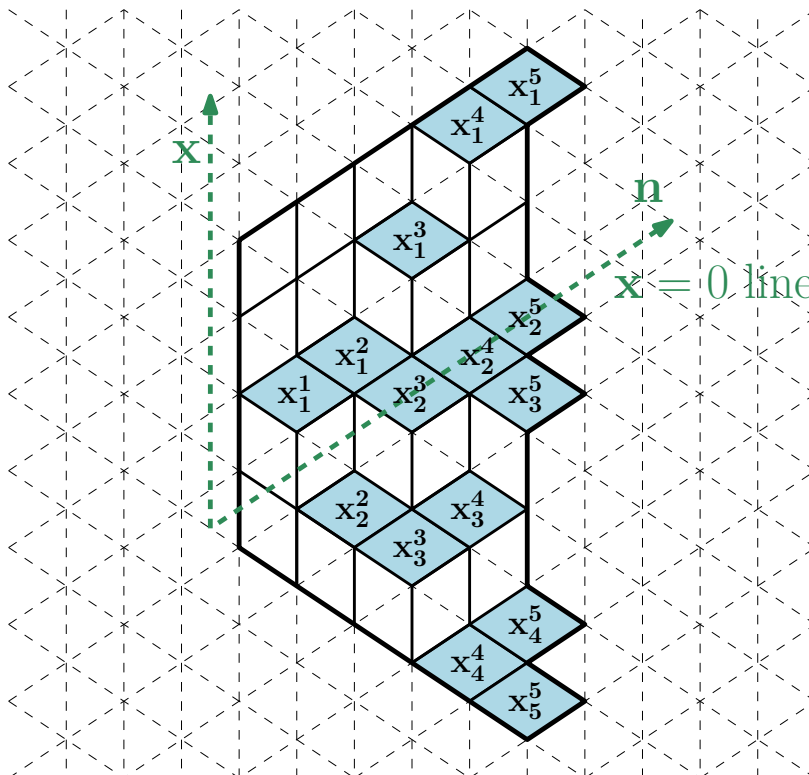


FIGURE 5. A lozenge tiling corresponding to a Gelfand–Tsetlin pattern with $N = 5$ and top row $x^5 = \mathbf{t} = (3, 0, -1, -4, -5)$.

²Note that in many articles an alternative parameterization $y_j^i = x_j^i + j$ is used. We stick to the notations of [Pe1], as we use many ideas from that paper.

In this section we investigate the asymptotic behavior of *uniformly random* Gelfand–Tsetlin patterns with fixed top row as $N \rightarrow \infty$. We adapt important ideas from [Pe1]; yet the results of that article are not enough for our purposes, so we need to generalize them and supplement with new considerations.

The following theorem of [Pe1] is our starting point, see also [DM].

Theorem 2.1 ([Pe1, Theorem 5.1]). *Fix an N -tuple of integers $\mathbf{t} = (\mathbf{t}_1 > \mathbf{t}_2 > \dots > \mathbf{t}_N)$, and let $\{x_i^j\}$, $1 \leq i \leq j \leq N$ be uniformly random Gelfand–Tsetlin pattern with top row \mathbf{t} . Then for any k and any collection of distinct pairs of integers $(x(1), n(1)), \dots, (x(k), n(k))$ with $1 \leq n(i) < N$, $i = 1, \dots, k$, we have*

$$\text{Prob} \left[x(i) \in \{x_1^{n(i)}, x_2^{n(i)}, \dots, x_j^{n(i)}\}, i = 1, \dots, k \right] = \det_{i,j=1}^k [K(x(i), n(i); x(j), n(j))],$$

where

$$(2.1) \quad K(x_1, n_1; x_2, n_2) = -\mathbf{1}_{n_2 < n_1} \mathbf{1}_{x_2 \leq x_1} \frac{(x_1 - x_2 + 1)_{n_1 - n_2 - 1}}{(n_1 - n_2 - 1)!} + \frac{(N - n_1)!}{(N - n_2 - 1)!} \\ \times \frac{1}{(2\pi\mathbf{i})^2} \oint_{\mathcal{C}(x_2, \dots, \mathbf{t}_1 - 1)} dz \oint_{\mathcal{C}(\infty)} dw \frac{(z - x_2 + 1)_{N - n_2 - 1}}{(w - x_1)_{N - n_1 + 1}} \frac{1}{w - z} \prod_{r=1}^N \frac{w - \mathbf{t}_r}{z - \mathbf{t}_r},$$

the contour $\mathcal{C}(x_2, \dots, \mathbf{t}_1 - 1)$ encloses points $x_2, x_2 + 1, \dots, \mathbf{t}_1 - 1$ and no other singularities of the integrand, and the contour $\mathcal{C}(\infty)$ is a very large circle; both contours have positive orientation.

The content of this section is the asymptotic analysis of the correlation kernel (2.1). Although we use a somewhat standard steepest descent approach to such analysis (cf. [O], [BG2], [Pe1]), but the technical details are delicate, as we need to deal with arbitrary N -tuples \mathbf{t} .

We start by rewriting the integrand in the double integral of (2.1) as

$$\frac{1}{w - z} \cdot \frac{1}{(w - x_1)(z - x_2 + N - n_2)} \cdot \exp(G_2(z) - G_1(w))$$

with

$$(2.2) \quad G_\kappa(z) = \sum_{a=1}^{N-n_\kappa} \ln(z - x_\kappa + a) - \sum_{r=1}^N \ln(z - \mathbf{t}_r), \quad \kappa = 1, 2.$$

Let us analyze the zeros of the derivative of $G_\kappa(z)$, i.e. the solutions to

$$(2.3) \quad \sum_{a=1}^{N-n_\kappa} \frac{1}{z - x_\kappa + a} = \sum_{r=1}^N \frac{1}{z - \mathbf{t}_r}$$

Lemma 2.2. *The equation (2.3) has either 0 or 2 non-real roots. In the latter case the non-real roots are complex conjugate to each other.*

Proof. Set $\mathbf{T} = \{\mathbf{t}_1, \mathbf{t}_2, \dots, \mathbf{t}_N\}$ and $\bar{\mathbf{T}} = \mathbb{Z} \setminus \mathbf{T}$. Then (2.3) can be written in the form

$$(2.4) \quad \sum_{d \in \mathbf{T} \setminus [x_\kappa - N + n_\kappa, x_\kappa - 1]} \frac{1}{z - d} - \sum_{d' \in \bar{\mathbf{T}} \cap [x_\kappa - N + n_\kappa, x_\kappa - 1]} \frac{1}{z - d'} = 0$$

Let M denote the total number of terms in (2.4). Then after clearing the denominators, the equation (2.4) becomes a polynomial equation of degree $M - 1$. Since all the

coefficients of this equation are real, all its non-real roots split into complex-conjugate pairs. We will now show that (2.4) has at least $M - 3$ real roots, which then implies that there is at most one complex conjugate pair.

Let $d_1^l < \dots < d_L^l$ be those elements of \mathbf{T} which are smaller than $x_\kappa - N + n_\kappa$ and let $d_1^r < \dots < d_R^r$ be those which are greater than $x_\kappa - 1$. Also let $d_1^l < \dots < d_P^l$ be elements of $\overline{\mathbf{T}} \cap [x_\kappa - N + n_\kappa, x_\kappa - 1]$. Clearly, $L + R + P = M$. Further, for each $i = 1, 2, \dots, L - 1$ the function (2.4) continuously changes from $+\infty$ to $-\infty$ on the real interval (d_i^l, d_{i+1}^l) and therefore has a zero on this interval. Similarly, there is a zero on each interval (d_i^r, d_{i+1}^r) , $i = 1, \dots, R - 1$ and on each interval (d_i^l, d_{i+1}^l) , $i = 1, \dots, P - 1$. Summing up, we found $(L - 1) + (R - 1) + (P - 1) = M - 3$ distinct real roots of (2.4). \square

We will further stick to the case when (2.4) has a pair of non-real roots (the asymptotic analysis in the case when all roots are real is more delicate and is left out of the scope of the present paper) and denote these roots τ_κ and $\bar{\tau}_\kappa$ with convention $\Im(\tau_\kappa) > 0$. Let us state the main result of this section.

Theorem 2.3. *Fix an arbitrary real parameter $D > 0$. Assume that the pairs (x_1, n_1) and (x_2, n_2) are such that the complex critical points τ_1 and τ_2 of $G_1(z)$ and $G_2(z)$, respectively, satisfy $\Im(\tau_{1,2}) > D^{-1}N$ and $|\tau_{1,2}| < DN$. Further, assume $|x_1 - x_2| + |n_1 - n_2| < D$ and that the points $\mathbf{t}_1, \dots, \mathbf{t}_N$ satisfy $\sum_{i=1}^N \ln^{1+1/D}(1 + |\mathbf{t}_i|/N) < DN$. Then the kernel (2.1) satisfies*

$$(2.5) \quad K(x_1, n_1; x_2, n_2) = \frac{(1 - n_1/N)^{1+n_2-n_1}}{2\pi\mathbf{i}} \int_{N^{-1}\bar{\tau}_1}^{N^{-1}\tau_1} \frac{(u - x_1/N)^{x_2-x_1-1}}{(u - x_1/N + 1 - n_1/N)^{x_2-x_1+n_2-n_1+1}} du + o(1),$$

where $o(1)$ is the uniformly small remainder as $N \rightarrow \infty$, and the integration contour crosses the real axis to the right from x_1/N when $n_2 \geq n_1$, and on the interval $(\frac{x_1+n_1-1}{N}, \frac{x_1}{N})$ when $n_2 < n_1$.

Remark 2.4. The change of variables $w = \frac{u-x_1/N}{u-x_1/N+1-n_1/N}$, i.e. $u = \frac{1-n_1/N}{1-w} + x_1/N + n_1/N - 1$ transforms the leading asymptotic of (2.5) into

$$(2.6) \quad \frac{1}{2\pi\mathbf{i}} \int_{\bar{\xi}}^{\xi} w^{x_2-x_1-1} (1-w)^{n_2-n_1} dw,$$

where the integration contour intersects the real line inside $(0, 1)$ when $n_2 \geq n_1$ and inside $(-\infty, 0)$ otherwise;

$$\xi = \frac{\tau_1/N - x_1/N}{\tau_1/N - x_1/N + 1 - n_1/N}.$$

The form (2.6) is known as the incomplete Beta-kernel.

In the rest of this section we prove Theorem 2.3.

The level lines of functions $\Re G_\kappa(z)$ and $\Im G_\kappa(\tau)$ passing through τ_κ , $\kappa = 1, 2$, are important for what follows, they are schematically sketched in Figure 6.

Let us explain the key features of Figure 6. Since τ_κ and $\bar{\tau}_\kappa$ are simple critical points of $G_\kappa(z)$ (i.e. $G_\kappa''(\tau_\kappa) \neq 0$, $G_\kappa''(\bar{\tau}_\kappa) \neq 0$) there are four branches of $\Re G_\kappa(z) = \text{const}$ and four branches of $\Im G_\kappa(z) = \text{const}$ going out of each critical point and these two kinds of branches interlace.

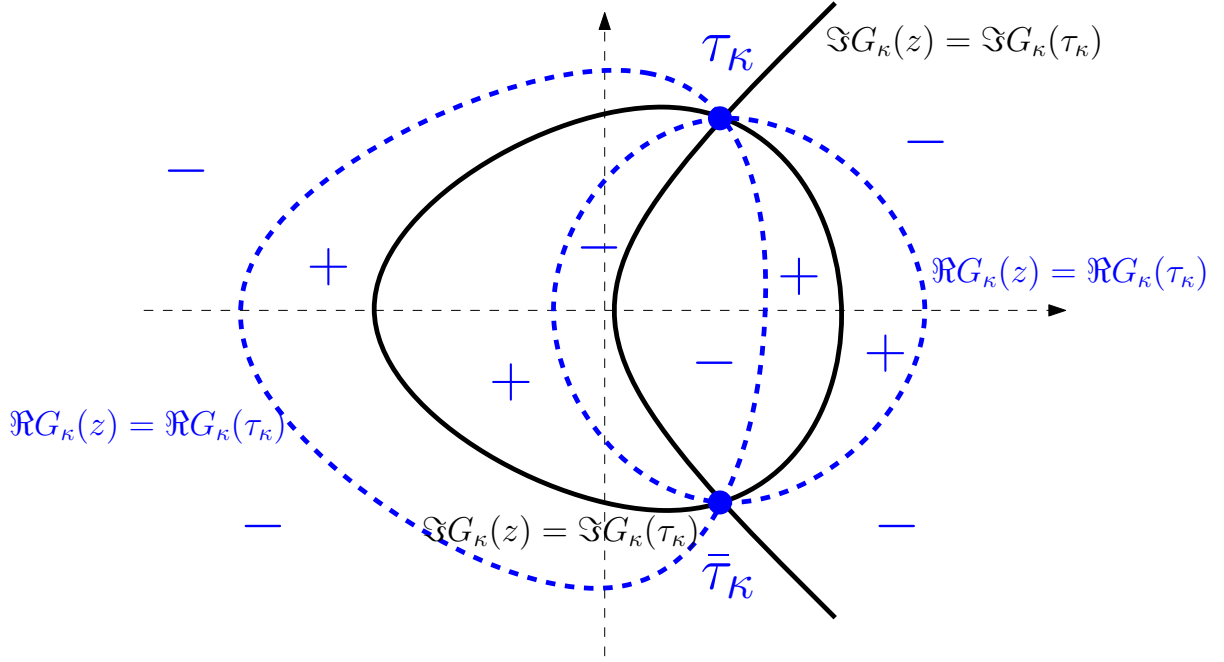


FIGURE 6. Contours $\Re G_\kappa(z) = \Re G_\kappa(\tau_\kappa)$, $\Im G_\kappa(z) = \Im G_\kappa(\tau_\kappa)$ going through $\tau_\kappa, \bar{\tau}_\kappa$. Pluses and minuses indicate the sign of $\Re(G_\kappa(z) - G_\kappa(\tau_\kappa))$ in each domain.

Since $\Re(G_\kappa(z)) \rightarrow -\infty$ as $z \rightarrow \infty$ the level lines of $\Re G_\kappa(z)$ are closed curves. These level lines can not intersect in a non-real point except at $\tau_\kappa, \bar{\tau}_\kappa$, as such an intersection would have been another critical point for $G_\kappa(z)$. Further, since $\Re G_\kappa(z)$ is harmonic everywhere outside the singularities on the real axis, each of its closed level lines must have one of these singularities inside. Finally, $\Re(G_\kappa(z)) = \Re(G_\kappa(\bar{z}))$ and therefore, the level lines are symmetric. Combination of these properties implies that there are four non-intersecting curves of constant $\Re G_\kappa(z)$ joining τ_κ with $\bar{\tau}_\kappa$, as in Figure 6.

Let us now in addition draw all other level lines $\Re G_\kappa(z) = \Re G_\kappa(\tau_\kappa)$; there might be no others in addition to the 4 we just drawn, but also there might be some additional loops near the real axis.

We would like to distinguish four regions on the plane bounded by level lines of $\Re G_\kappa(z)$; these are 4 regions adjacent to τ_κ . (Note that, in principle, these four regions do not have to cover the whole plane, but we know that each of them contains some points of the real axis). One of these regions is unbounded, while the other two are bounded and we call them left, middle and right (according to the position of their intersections with the real axis) Due to the maximum principle for the harmonic functions and the behavior at the infinity of $\Re(G_\kappa(z))$ in the exterior (infinite) region we have $\Re G_\kappa(z) < \Re G_\kappa(\tau_\kappa)$. Therefore, since τ_κ is a simple critical point for $G_\kappa(z)$, also $\Re G_\kappa(z) < \Re G_\kappa(\tau_\kappa)$ in the middle bounded region, and $\Re G_\kappa(z) > \Re G_\kappa(\tau_\kappa)$ in both left and right bounded regions.

We will further distinguish four contours. $C_\kappa^{(m)}$ is the curve $\Im(G_\kappa(z)) = \Im(\tau_\kappa)$ which starts at τ_κ and continues in the middle bounded region until it reaches the real axis. After that we continue the curve symmetrically to $\bar{\tau}_\kappa$. Note that $\Re(G_\kappa(z))$ is monotonous along $C_\kappa^{(m)}$ except, perhaps, at the real axis, since its local extremum would necessary be a critical point. Therefore, $\Re(G_\kappa(z))$ monotonously decreases as we move away from τ_κ in the upper half-plane and increases as we move towards $\bar{\tau}_\kappa$

in the lower halfplane. Also observe that the choice of the branch of the logarithm in (2.2) is not important here as the curve $C_\kappa^{(m)}$ is constructed locally and therefore does not depend on this choice.

Further, $C_\kappa^{(r)}$ is the curve $\Im(G_\kappa(z)) = \Im(\tau_\kappa)$ which starts at τ_κ and continues in the right bounded region until it reaches the real axis. After that we continue the curve symmetrically to $\bar{\tau}_\kappa$. Along this curve $\Re(G_\kappa(z))$ monotonously increases as we move away from τ_κ in the upper half-plane and decreases as we move towards $\bar{\tau}_\kappa$ in the lower halfplane.

The contour $C_\kappa^{(l)}$ is defined in the same way, but inside the left bounded region.

The contour $C_\kappa^{(i)}$ is the curve $\Im(G_\kappa(z)) = \Im(\tau_\kappa)$ which starts at τ_κ and continues in the infinite region. This curve will never go back to the real axis (this is established below by counting the points on the real axis where $\Im(G_\kappa(z)) = \Im(\tau_\kappa)$) and thus goes to infinity in the upper half-plane. We then return symmetrically from the infinity to $\bar{\tau}_\kappa$ in the lower half-plane.

Lemma 2.5. *The curve $C_\kappa^{(m)}$ intersects the real axis inside the interval $(x_\kappa + n_\kappa - N, x_\kappa - 1)$, and the curve $C_\kappa^{(i)}$ does not intersect the real axis. The curve $C_\kappa^{(l)}$ intersects the real axis to the left from $x_\kappa + n_\kappa - N$, and the curve $C_\kappa^{(r)}$ intersects the real axis to the right from $x_\kappa - 1$.*

Proof. Choose a small positive parameter $\varepsilon > 0$ and let γ be the curve which is the real axis, except near the singularities of $G(z)$ (i.e. the points d and d' in (2.4)). γ walks around each singularity by a half-circle in the upper-halfplane centered at this singularity and of the radius ε .

We remarked above that the curves $C_\kappa^{(m)}$, $C_\kappa^{(r)}$, $C_\kappa^{(l)}$, and $C_\kappa^{(i)}$ do not depend on the choice of branches of the logarithm in (2.2). But we need to choose *some* branch and so we use the branch of $\ln(y)$ with a cut along the negative *imaginary* axis in terms of y and such that the value at positive real y is real. With this notation in mind, let us trace the values of $\Im(G_\kappa(z))$ along the curve γ moving in the direction of growing x . Clearly, if we choose ε small enough, then $\Im(G_\kappa(z))$ is constant on straight segments between the singularities, increases along the half-circles corresponding to singularities d in (2.4) and decreases along the half-circles corresponding to singularities d' in (2.4). At $+\infty$ the value of this function is 0. This is schematically illustrated in Figure 7.

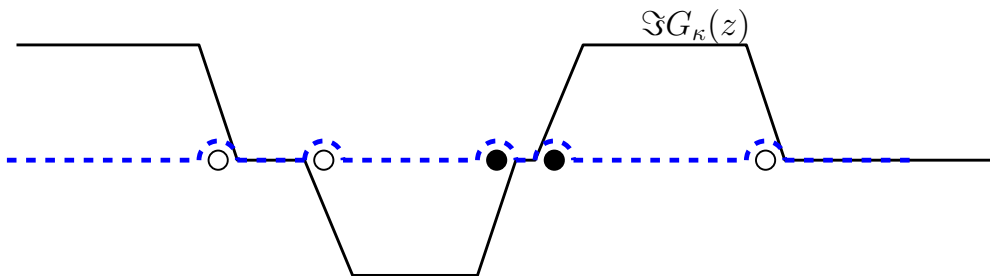


FIGURE 7. Imaginary part (in solid black) of $G_\kappa(z)$ along the (blue dashed) curve which follows the real line avoiding the singularities. White points correspond to d terms in the first sum of (2.4) and black points correspond to d' terms in the second sum.

At a point z where one of our curves intersects the real axis we should have $\Im(G_\kappa(z)) = \Im(G_\kappa(\tau_\kappa))$. We claim that there can not be two intersections on the same

horizontal segment of the graph of $\Im(G_\kappa(z))$ along τ . Indeed, each such intersection is a critical point of $G_\kappa(z)$ (since the real axis itself is also a level line $\Im(G_\kappa(z)) = \text{const}$), but the analysis of critical points in the proof of Lemma 2.2 shows that there are never more than one critical points between two real singularities of G_κ . Also these curves can not intersect the real axis on the segments (d_L^l, d_1^l) and (d_P^r, d_1^R) — because we know that there are no critical points of G_1 on these segments.

Therefore, our curves can not have more than 3 intersections with real axis, and, thus, they have exactly three, in particular, $G_\kappa^{(i)}$ does not intersect the real axis. The middle intersection then belongs to $G_\kappa^{(m)}$ and should be in the interval $[d_1^l, d_P^r] \subset (x_\kappa + n_\kappa - N, x_\kappa - 1)$. The right intersection belongs to $G_\kappa^{(r)}$ and should be in the interval $[d_1^r, +\infty) \subset (x_\kappa - 1, +\infty)$. Finally, the left intersection belongs to $G_\kappa^{(l)}$ and should be in the interval $(-\infty, d_L^l] \subset (-\infty, x_\kappa + n_\kappa - N)$. \square

Next, we need analogues of Lemmas 2.2, 2.5, in which the point configuration \mathbf{t} is replaced by a probability measure. Take a probability density $\nu(x)$, $x \in \mathbb{R}$ such that $\nu(x) \leq 1$ for all x , and two numbers, $\mathbf{x} \in \mathbb{R}$, $0 < \boldsymbol{\eta} < 1$. Given this data, define

$$(2.7) \quad G(z) = \int_{\mathbf{x} + \boldsymbol{\eta} - 1}^{\mathbf{x}} \ln(z - t) dt - \int_{\mathbb{R}} \ln(z - y) \nu(y) dy.$$

Lemma 2.6. *The equation $G'(z) = 0$ has either 0 or 2 non-real roots. In the latter case the non-real roots are complex conjugate to each other.*

Proof. The function $G(z)$ outside the real axis can be (uniformly on the compact subsets of $\mathbb{C} \setminus \mathbb{R}$) approximated by functions of the form $\frac{1}{N} G_\kappa(z)$ of (2.2). It remains to combine Lemma 2.2 with Rouché's theorem. \square

Suppose that $G'(z) = 0$ has two complex roots, and let τ denote the root in the upper half-plane. Define four curves $C^{(m)}$, $C^{(l)}$, $C^{(r)}$, $C^{(i)}$ in the same way as $C_\kappa^{(m)}$, $C_\kappa^{(l)}$, $C_\kappa^{(r)}$, $C_\kappa^{(i)}$, i.e. they are parts of the lines $\Im(G_\kappa(z)) = \Im(\tau_\kappa)$ in the upper half-plane continued symmetrically to the lower half-plane.

Lemma 2.7. *The curve $C^{(m)}$ intersects the real axis inside the interval $(\mathbf{x} + \boldsymbol{\eta}_\kappa - 1, \mathbf{x})$, and the curve $C^{(i)}$ does not intersect the real axis. The curve $C^{(l)}$ intersects the real axis to the left from $\mathbf{x} + \boldsymbol{\eta} - 1$, and the curve $C^{(r)}$ intersects the real axis to the right from \mathbf{x} .*

Proof. The proof follows the same lines as that of Lemma 2.5. In more details, we trace the imaginary part of $G(z)$ along the curve $\Im(z) = \varepsilon > 0$. \square

The last technical ingredient needed for the proof of Theorem 2.3 is the following statement.

Lemma 2.8. *For $N = 1, 2, \dots$, set*

$$R_N(x) = \sum_{k=-N}^N \left| \frac{1}{ix + 1/2 + k} \right| = \sum_{k=-N}^N \frac{1}{\sqrt{x^2 + (k + 1/2)^2}}.$$

Then

$$\lim_{\varepsilon \rightarrow 0} \limsup_{N \rightarrow \infty} \frac{1}{N} \int_0^{N\varepsilon} R_N(x) dx = 0.$$

Proof. Integrating $R_N(x)$ termwise we get

$$(2.8) \quad \int_0^{N\varepsilon} R_N(x) dx = \sum_{k=-N}^N \operatorname{arcsch} \left(\frac{\varepsilon N}{|k + 1/2|} \right),$$

where $\operatorname{arcsch}(x)$ is the inverse functions to $\sinh(x) = \frac{e^x - e^{-x}}{2}$, i.e.

$$\operatorname{arcsch}(x) = \ln \left(x + \sqrt{x^2 + 1} \right), \quad x \geq 0.$$

Split the sum in (2.8) into two: the first one has k such that $|k + 1/2| > \sqrt{\varepsilon}N$ and the second one is the rest. The first sum is bounded from above by

$$(2.9) \quad (2N + 1) \operatorname{arcsch}(\sqrt{\varepsilon}).$$

For the second sum we use the inequality

$$\operatorname{arcsch}(x) = \ln(x) + \ln \left(1 + \sqrt{1 + 1/x^2} \right) \leq \ln(x) + \ln \left(\frac{3}{\sqrt{\varepsilon}} \right), \quad x > \sqrt{\varepsilon}, \quad 0 < \varepsilon < 1,$$

which gives the bound

$$(2.10) \quad \sum_{|k+1/2| \leq \sqrt{\varepsilon}N} \operatorname{arcsch} \left(\frac{\varepsilon N}{|k + 1/2|} \right) \leq \sum_{|k+1/2| < \sqrt{\varepsilon}N} \left(\ln(\varepsilon) + \ln(N) - \ln |k + 1/2| + \ln \left(\frac{3}{\sqrt{\varepsilon}} \right) \right) \\ \leq (2\sqrt{\varepsilon}N + 1)(\ln(N) + \ln(3/\sqrt{\varepsilon})) - 2 \ln(\lfloor \sqrt{\varepsilon}N - 1 \rfloor!)$$

The Stirling's formula yields $\ln(x!) > x(\ln(x) - 1)$ for large x , and therefore, we further bound (2.10) by

$$(2.11) \quad (2\sqrt{\varepsilon}N + 1)(\ln(N) + \ln(3/\sqrt{\varepsilon})) - 2(\sqrt{\varepsilon}N - 2)(\ln(\sqrt{\varepsilon}N - 2) - 1) \\ \leq C(\ln(N) + \sqrt{\varepsilon}N + \sqrt{\varepsilon} \ln(1/\varepsilon)N + 1),$$

for a constant $C > 0$. Summing (2.9) and (2.10), dividing by N , sending $N \rightarrow \infty$ and then $\varepsilon \rightarrow 0$ we get the desired claim. \square

Proof of Theorem 2.3. We denote through μ_N the signed measure on \mathbb{R} describing the scaled by N points d and d' from (2.4):

$$(2.12) \quad \mu_N = \frac{1}{N} \sum_{d \in \mathbf{T} \setminus [x_1 - N + n_1, x_1 - 1]} \delta_{d/N} - \frac{1}{N} \sum_{d' \in \bar{\mathbf{T}} \cap [x_1 - N + n_1, x_1 - 1]} \delta_{d'/N}.$$

The assumption $\sum_{i=1}^N \ln^{1+1/D}(1 + |\mathbf{t}_i|/N) < DN$ implies that the measures μ_N are tight, and therefore by the standard compactness arguments we can (and will) assume that the measures μ_N weakly converge as $N \rightarrow \infty$ to a signed measure μ . Note that μ_N -mass of any interval $[a, b]$ is satisfies the bounds

$$a - b - \frac{1}{N} \leq \mu_N([a, b]) \leq b - a + \frac{1}{N},$$

therefore μ is an absolutely continuous signed measure with density $\mu(x)$ bounded between -1 and 1 .

Recall the functions $G_i(z)$ of (2.2), and let us introduce their normalized versions through:

$$\begin{aligned} G_1^{(N)}(u) &= \frac{1}{N} \sum_{d \in \mathbf{T} \setminus [x_1 - N + n_1, x_1 - 1]} \ln(u - d/N) - \frac{1}{N} \sum_{d' \in \overline{\mathbf{T}} \cap [x_1 - N + n_1, x_1 - 1]} \ln(u - d'/N) \\ &= \int_{\mathbb{R}} \ln(z - x) \mu_N(dx), \end{aligned}$$

and similarly for $G_2^{(N)}(u)$. Also set

$$G^\infty(z) = \int_{\mathbb{R}} \ln(z - x) \mu(x) dx,$$

which is well-defined due to the assumption $\sum_{i=1}^N \ln^{1+1/D}(1 + |\mathbf{t}_i|/N) < DN$, and note that the same assumption implies

$$G_1^{(N)}(z) \rightrightarrows G^\infty(z)$$

uniformly over z in compact subsets of $\mathbb{C} \setminus \{z \mid \Im(z) = 0\}$. Since the differences $|n_2 - n_1|$ and $|x_1 - x_2|$ stay finite as $N \rightarrow \infty$, we also have

$$G_2^{(N)}(z) \rightrightarrows G^\infty(z).$$

We now introduce two integration contours. For the \mathcal{C}_z contour we start from the union of $C_1^{(m)}$ and $C_1^{(i)}$ oriented from top to bottom. From the technical point of view it is convenient to modify this contour near the real axis³ Namely, we choose $\varepsilon > 0$ to be fixed later and assume that $\Re\tau_1 > \varepsilon N$. As soon as \mathcal{C}_z contour (recall that we are tracing it from the bottom) reached the level $\Im(z) = -\varepsilon N$, it immediately has a horizontal segment so that to turn $\Re(z)$ into a half-integer (i.e. number of the form $1/2 + n$, $n \in \mathbb{Z}$), and then vertical segment from $\Im(z) = -\varepsilon N$ to $\Im(z) = 0$. In the upper halfplane $\Im(z) > 0$ we do the same modification. Similarly, and \mathcal{C}_w is defined as the union of $C_2^{(r)}$ and $C_2^{(l)}$ oriented counter-clockwise and modified to a vertical line with half-integer real part for $-\varepsilon N < \Im(z) < \varepsilon N$. We refer to Figure 8 for an illustration.

Note that due to convergence $G_{1,2}^{(N)}(z) \rightrightarrows G^\infty(z)$, the contours do not oscillate as $N \rightarrow \infty$, but smoothly approximate similar contours constructed using $G^\infty(z)$.

We next deform the z and w contours in (2.1) into \mathcal{C}_z and \mathcal{C}_w , respectively. Lemmas 2.5, 2.7 imply that the only residues which we collect in this deformation are those coming from the $\frac{1}{w-z}$ pole. Let us first deform the z contour (there is no residue coming from $w = z$ at this stage, as w is very large), and then proceed to the w -contour. Therefore, the result of the deformation is the z -integral over a contour $\mathcal{C}_z^{def} \subset \mathcal{C}_z$, of the w -residue of the integrand in the double integral in (2.1) at point

³The subsequent proofs will probably go through even without this modification, but rigorous justifications of some steps would become more involved, due to the singularities of the integrand near the real axis.

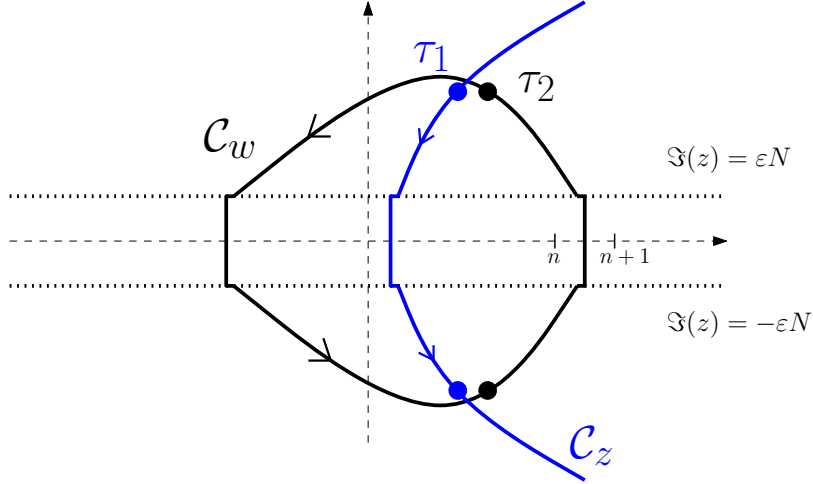


FIGURE 8. \mathcal{C}_z and \mathcal{C}_w contours, which are the level lines of $\Im(G_{1,2}(z))$ (cf. Figure 6) modified near the real axis.

$w = z$, i.e.

$$(2.13) \quad K(x_1, n_1; x_2, n_2) = -\mathbf{1}_{n_2 < n_1} \mathbf{1}_{x_2 \leq x_1} \frac{(x_1 - x_2 + 1)_{n_1 - n_2 - 1}}{(n_1 - n_2 - 1)!} \\ + \frac{(N - n_1)!}{(N - n_2 - 1)!} \frac{1}{2\pi\mathbf{i}} \int_{\mathcal{C}_z^{def}} \frac{dz}{(z - x_1)(z - x_2 + N - n_2)} \cdot \frac{\exp(G_2(z))}{\exp(G_1(z))} \\ + \frac{(N - n_1)!}{(N - n_2 - 1)!} \frac{1}{(2\pi\mathbf{i})^2} \oint_{\mathcal{C}_z} dz \oint_{\mathcal{C}_w} dw \frac{1}{w - z} \cdot \frac{1}{(w - x_1)(z - x_2 + N - n_2)} \cdot \frac{\exp(G_2(z))}{\exp(G_1(w))}.$$

Note that \mathcal{C}_z^{def} is passed from bottom to top and it intersects the real line to the right from x_1 .

The change of variables $u = z/N$, $v = w/N$ transforms the kernel $K(x_1, n_1; x_2, n_2)$ into the form

$$(2.14) \quad K(x_1, n_1; x_2, n_2) = -\mathbf{1}_{n_2 < n_1} \mathbf{1}_{x_2 \leq x_1} \frac{(x_1 - x_2 + 1)_{n_1 - n_2 - 1}}{(n_1 - n_2 - 1)!} \\ + \frac{(N - n_2)_{n_2 + 1} N^{n_1}}{(N - n_1 + 1)_{n_1} N^{n_2 + 1}} \frac{1}{2\pi\mathbf{i}} \int_{\mathcal{C}_u^{def}} \frac{du}{(u - x_1/N)(u - x_2/N + 1 - n_2/N)} \cdot \frac{\exp(NG_2^{(N)}(u))}{\exp(NG_1^{(N)}(u))} \\ + \frac{(N - n_2)_{n_2 + 1} N^{n_1}}{(N - n_1 + 1)_{n_1} N^{n_2 + 1}} \frac{1}{(2\pi\mathbf{i})^2} \oint_{\mathcal{C}_u} du \oint_{\mathcal{C}_v} \frac{dv}{v - u} \cdot \frac{1}{(v - \frac{x_1}{N})(u - \frac{x_2}{N} + 1 - \frac{n_2}{N})} \frac{\exp(NG_2^{(N)}(u))}{\exp(NG_1^{(N)}(v))},$$

where u and v contours are the contours of (2.13) rescaled by N . Note that since the functions $G_1^{(N)}$ and $G_2^{(N)}$ uniformly converge to G^∞ outside ε -neighborhood of the real line, and the contours are the level lines of the imaginary part of the former functions, they converge to similar level lines for G^∞ . In particular, the lengths of all the involved contours are bounded as $N \rightarrow \infty$, and \mathcal{C}_u might intersect with \mathcal{C}_v only in a neighborhood of τ_1/N .

Let us analyze the $N \rightarrow \infty$ behavior of each term in (2.14). The first line does not depend on N . For the second line observe that for $x_1 \geq x_2$, $n_1 \geq n_2$ we have

$$(2.15) \quad \frac{\exp(NG_2^{(N)}(u))}{\exp(NG_1^{(N)}(u))} = \frac{\prod_{a=1}^{N-n_1+(n_1-n_2)} \left(u - \frac{x_1}{N} + \frac{a}{N} + \frac{x_1-x_2}{N}\right)}{\prod_{a=1}^{N-n_1} \left(u - \frac{x_1}{N} + \frac{a}{N}\right)} \\ = \frac{\prod_{a=N-n_1+1}^{N-n_1+(n_1-n_2)+(x_1-x_2)} \left(u - \frac{x_1}{N} + \frac{a}{N}\right)}{\prod_{a=1}^{x_1-x_2} \left(u - \frac{x_1}{N} + \frac{a}{N}\right)}.$$

Due to Lemmas 2.5, 2.7 the integration contours are bounded away from the points $u = x_1/N$ and $u = (x_1 + n_1 - N)/N$. Therefore, (2.15) uniformly converges on the integration contours and thus the second line in (2.14) is as $N \rightarrow \infty$

$$\frac{(1 - n_1/N)^{1+n_2-n_1}}{2\pi i} \int_{\mathcal{C}_u^{def}} \frac{\left(u - \frac{x_1}{N}\right)^{x_2-x_1-1}}{\left(u - \frac{x_1}{N} + 1 - \frac{n_1}{N}\right)^{1+n_2-n_1+x_2-x_1}} du + o(1).$$

When $x_1 < x_2$ or $n_1 < n_2$ the computation is the same. Since the point of the intersection of the contours \mathcal{C}_u and \mathcal{C}_v approaches τ_1/N as $N \rightarrow \infty$, the final asymptotic for the second line of (2.14) is

$$(2.16) \quad \frac{(1 - n_1/N)^{1+n_2-n_1}}{2\pi i} \int_{\bar{\tau}_1/N}^{\tau_1/N} \frac{\left(u - \frac{x_1}{N}\right)^{x_2-x_1-1}}{\left(u - \frac{x_1}{N} + 1 - \frac{n_1}{N}\right)^{1+n_2-n_1+x_2-x_1}} du + o(1),$$

where the integration contour crosses the real axis to the right from $\frac{x_1}{N}$.

Now we turn to the third line in (2.14). Fix any $\delta > 0$. We claim that outside the δ -neighborhood of the points τ_1/N , $\bar{\tau}_1/N$ the integrand is exponentially (in N) small. Indeed, by the construction of the contours, $\Re(G_2^{(N)}(u))$ (strictly) decreases as we move away from the point τ_2/N (similarly with $\bar{\tau}_2/N$) as long as we do not get into the ε -neighborhood of the real axis. Lemma 2.8 gives a uniform bound for the derivative of $G_2^{(N)}(u)$ near the real axis, which shows, that $\Re(G_2^{(N)}(u))$ can not grow much near the real axis.

In the same way $\Re(G_1^{(N)}(u))$ increases as we move away from τ_1/N and does not grow much near the real axis, where monotonicity no longer holds.

On the other hand for small values of δ , we can Taylor expand $G_1^{(N)}(u)$ and $G_2^{(N)}(u)$ near the points τ_1/N , τ_2/N , respectively. Since $G_i^{(N)}(u)$ uniformly converges to $G^\infty(u)$, we essentially deal with the Taylor expansion of the latter function. Since τ_1/N , τ_2/N are critical points of the corresponding functions, we have

$$(2.17) \quad \exp(N(G_2^{(N)}(u) - G_1^{(N)}(v))) = \exp(N(G_2^{(N)}(\tau_2/N) - G_1^{(N)}(\tau_1/N))) \\ \times \exp\left(N\left((G_2^{(N)})''(\tau_2/N)(u - \tau_2/N)^2 - (G_1^{(N)})''(\tau_1/N)(v - \tau_1/N)^2 + O(|u - \tau_2/N|^3 + |v - \tau_1/N|^3)\right)\right)$$

Since the difference $G_1^{(N)}(u) - G_2^{(N)}(u)$ is (uniformly) of order $1/N$ as $N \rightarrow \infty$, the factor $\exp(N(G_2^{(N)}(\tau_2/N) - G_1^{(N)}(\tau_1/N)))$ stays bounded as $N \rightarrow \infty$. Turning to the second line in (2.17), note that by the definition, the tangent to the \mathcal{C}_u contour at τ_1/N is such that on this tangent $(G_2^{(N)})''(\tau_2/N)(u - \tau_2/N)^2$ is negative real and the tangent to the \mathcal{C}_v contour at τ_2/N is such that $(G_1^{(N)})''(\tau_1/N)(v - \tau_1/N)^2$ is positive

real. Therefore, the integral (over δ -neighborhood of τ_1/N , along our contours) in the third line of (2.14) decays as $N \rightarrow \infty$ (in fact, it behaves as $O(N^{-1/2})$).

Summing up, (2.14) behaves when $N \rightarrow \infty$ as

$$(2.18) \quad K(x_1, n_1; x_2, n_2) = -\mathbf{1}_{n_2 < n_1} \mathbf{1}_{x_2 \leq x_1} \frac{(x_1 - x_2 + 1)_{n_1 - n_2 - 1}}{(n_1 - n_2 - 1)!} \\ + \frac{(1 - n_1/N)^{1+n_2-n_1}}{2\pi\mathbf{i}} \int_{\bar{\tau}_1/N}^{\tau_1/N} \frac{\left(u - \frac{x_1}{N}\right)^{x_2 - x_1 - 1}}{\left(u - \frac{x_1}{N} + 1 - \frac{n_1}{N}\right)^{1+n_2-n_1+x_2-x_1}} du + o(1),$$

where the integration contour crosses the real axis to the right from $\frac{x_1}{N}$.

We claim that when $n_2 < n_1$, $x_2 \leq x_1$, then the first term in (2.18) is precisely the minus residue of the second term at $u = x_1/N$. Indeed, from one side

$$\frac{(x_1 - x_2 + 1)_{n_1 - n_2 - 1}}{(n_1 - n_2 - 1)!} = \frac{(x_1 - x_2 + n_1 - n_2 - 1)!}{(x_1 - x_2)!(n_1 - n_2 - 1)!}.$$

On the other side,

$$(2.19) \quad \text{Res}_{u=\frac{x_1}{N}} \left[\frac{\left(u - \frac{x_1}{N} + 1 - \frac{n_1}{N}\right)^{n_1 - n_2 + x_1 - x_2 - 1}}{\left(u - \frac{x_1}{N}\right)^{x_1 - x_2 + 1}} \right] \\ = \frac{1}{(x_1 - x_2)!} \left(\frac{\partial}{\partial u} \right)^{x_1 - x_2} \left(u - \frac{x_1}{N} + 1 - \frac{n_1}{N} \right)^{n_1 - n_2 + x_1 - x_2 - 1} \Big|_{u=x_1/N} \\ = \frac{(n_1 - n_2 + x_1 - x_2 - 1)!}{(x_1 - x_2)!(n_1 - n_2 - 1)!} \left(1 - \frac{n_1}{N} \right)^{n_1 - n_2 - 1}.$$

We conclude that

$$(2.20) \quad K(x_1, n_1; x_2, n_2) = \frac{(1 - n_1/N)^{1+n_2-n_1}}{2\pi\mathbf{i}} \int_{\bar{\tau}_1/N}^{\tau_1/N} \frac{\left(u - \frac{x_1}{N}\right)^{x_2 - x_1 - 1}}{\left(u - \frac{x_1}{N} + 1 - \frac{n_1}{N}\right)^{1+n_2-n_1+x_2-x_1}} du + o(1),$$

where the integration contour crosses the real axis to the right from x_1/N when $n_2 \geq n_1$ and inside the interval $(\frac{x_1+n_1-1}{N}, \frac{x_1}{N})$ otherwise. \square

3. LAW OF LARGE NUMBERS FOR TILINGS

Take a lozenge tiling of an arbitrary *simply-connected* domain on a regular triangular grid. We aim to define for each vertex \mathbf{v} of the grid inside the domain the value of *height function* $H(\mathbf{v})$. For that we choose two types of lozenges out of three (we have chosen *non-horizontal* ones, see Figure 9) and draw their middle lines, thus arriving at a family of non-intersecting paths corresponding to the tiling. The value of the height function increases by 1 when we cross such a path (from bottom to top), this condition defines the values of $H(\cdot)$ up to an addition of an arbitrary constant. We fix this constant by a convention that H vanishes at the bottom point of the left-most vertical of the domain, see Figure 9.

Observe that along the boundary of the domain, the values of the height function do not depend on the choice of lozenge tiling. Indeed, the height function changes linearly along the vertical segments of the boundary and is constant along two other types of boundary segments.

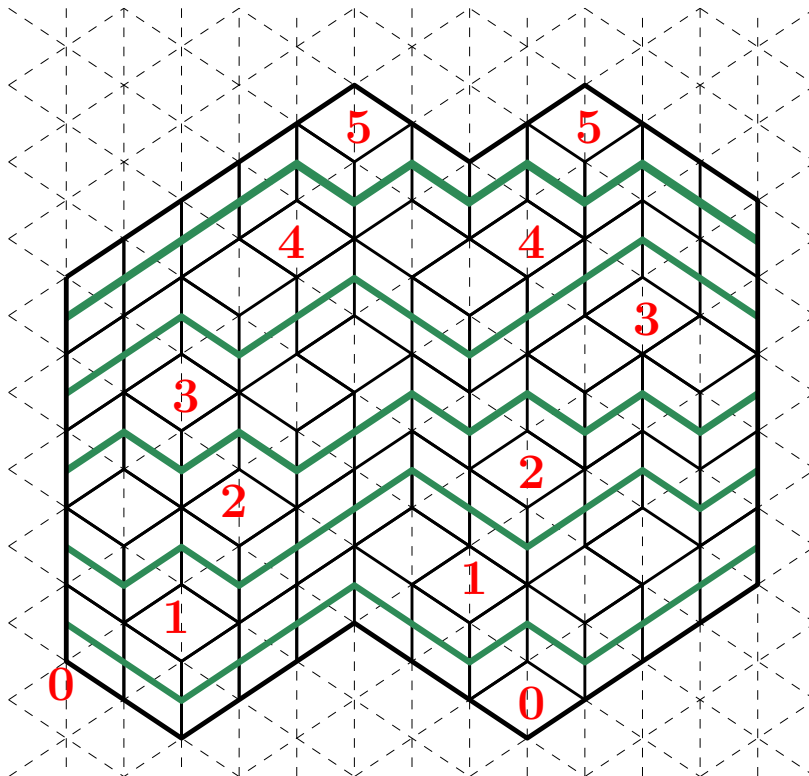


FIGURE 9. Height function of a lozenge tiling.

Let Ω_L , $L = 1, 2, \dots$, be a sequence of simply-connected domains on the triangular grid such that each Ω_L has at least one lozenge tiling. Further, let Ω be a simply-connected domain with piecewise-smooth boundary $\partial\Omega$, and let h be a continuous real function on $\partial\Omega$.

For two sets $A, B \subset \mathbb{R}^k$ we say that they are within ε -distance from each other, if for each $x \in A$ there exists $y \in B$ such that $\text{dist}(x, y) < \varepsilon$, and for each $y \in B$ there exists $x \in A$, such that $\text{dist}(x, y) < \varepsilon$. Here $\text{dist}(\cdot, \cdot)$ is the Euclidian distance.

We say that Ω_L approximates (Ω, h) as $L \rightarrow \infty$, if $\frac{1}{L}\Omega_L \subset \Omega$ for each L , and for each $\varepsilon > 0$ the set $(\partial\Omega, h) = \{(x, y) \in \mathbb{R}^2 \times \mathbb{R} \mid x \in \partial\Omega, y = h(x)\}$ becomes within ε -distance of $(\frac{1}{L}\partial\Omega_L, \frac{1}{L}H_{\Omega_L})$ as $L \rightarrow \infty$. Here H_{Ω_L} is the height function of lozenge tilings of Ω_L on $\partial\Omega_L$.

Theorem 3.1. *Suppose that the domains Ω_L approximate (Ω, h) as $L \rightarrow \infty$. Then the rescaled height function $\frac{1}{L}H_L(\mathbf{x}L, \mathbf{y}L)$ of uniformly random lozenge tiling of Ω_L converges in uniform norm, in probability to a non-random function H_Ω on Ω , which coincides with h on $\partial\Omega$.*

The proof of Theorem 3.1 is given in [CKP], see also [CEP], [KOS]. The function H_Ω is identified there with a solution to a certain variational problem and therefore depends only on Ω and h . More direct descriptions for restrictive classes of domains Ω were given in [KO] and [BuG1]. The function H_Ω is always Lipschitz, but its derivatives might have discontinuities, e.g. at the points where the inscribed circle is tangent to the hexagon in Figure 1.

Theorem 3.1 can be reinterpreted as the Law of Large Numbers for the average proportions of lozenges of three types. The definition of the height function implies

that the derivatives of H_Ω in up-left and up-right grid directions correspond to average densities of two types of lozenges: p^\blacktriangledown and p^\blacktriangleright , respectively, see Figure 10. The third density is then also reconstructed from directional derivatives, e.g. using $p^\diamond = 1 - p^\blacktriangledown - p^\blacktriangleright$. Therefore, the limit shape $H_\Omega(x, y)$ can be encoded by 3 functions $p^\blacktriangledown(x, y)$, $p^\blacktriangleright(x, y)$, and $p^\diamond(x, y)$, which sum up to identical 1. Then Theorem 3.1 yields that for any subdomain $\mathcal{D} \subset \Omega$ the numbers of lozenges (inside $L\mathcal{D}$ in uniformly random lozenge tiling of Ω_L) of three types divided by L converges as $L \rightarrow \infty$, in probability, to the integrals over \mathcal{D} of these three functions, as in Theorem 1.1.

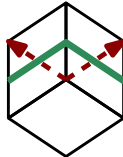


FIGURE 10. Derivatives in grid directions correspond to proportions of lozenges.

4. BULK LIMITS

In this section we prove the main results announced in the introduction. Theorem 1.1 is a combination of Theorems 4.1 and 4.3. Theorem 4.5 is a refinement of Corollary 1.2.

For a probability measure ν on \mathbb{R} with bounded by 1 density $\nu(x)$, and two parameters $\mathbf{x} \in \mathbb{R}$, $0 < \boldsymbol{\eta} < 1$ we define a function $G_{\nu, \mathbf{x}, \boldsymbol{\eta}}(z)$ through the formula (2.7). It is an analytic function on $\mathbb{C} \setminus \mathbb{R}$ with derivative given by

$$G'_{\nu, \mathbf{x}, \boldsymbol{\eta}}(z) = \int_{\mathbf{x} + \boldsymbol{\eta} - 1}^{\mathbf{x}} \frac{dt}{z - t} - \int_{\mathbb{R}} \frac{1}{z - y} \nu(y) dy = \ln(z + 1 - \mathbf{x} - \boldsymbol{\eta}) - \ln(z - \mathbf{x}) - \int_{\mathbb{R}} \frac{1}{z - y} \nu(y) dy$$

According to Lemma 2.6, the equation $G'_{\nu, \boldsymbol{\eta}, \mathbf{x}}(z) = 0$ has at most 1 solution $z = \tau(\nu, \mathbf{x}, \boldsymbol{\eta})$ in the upper half-plane. Denote

$$\xi(\nu, \mathbf{x}, \boldsymbol{\eta}) = \frac{\tau(\nu, \mathbf{x}, \boldsymbol{\eta}) - \mathbf{x}}{\tau(\nu, \mathbf{x}, \boldsymbol{\eta}) + 1 - \mathbf{x} - \boldsymbol{\eta}},$$

and note that when τ is in the upper half-plane, then so is ξ . We will say that $\xi(\nu, \mathbf{x}, \boldsymbol{\eta})$ is *well-defined*, if the equation $G'_{\nu, \mathbf{x}, \boldsymbol{\eta}}(z)$ has a non-real solution.

Given a complex number ξ with positive imaginary part the *incomplete Beta kernel* (see [OR], [KOS]) is defined through

$$(4.1) \quad K_\xi(x_1, n_1; x_2, n_2) = \frac{1}{2\pi\mathbf{i}} \int_{\bar{\xi}}^{\xi} w^{x_2 - x_1 - 1} (1 - w)^{n_2 - n_1} dw,$$

where the integration contour crosses the real line inside $(0, 1)$ for $n_2 \geq n_1$ and inside $(-\infty, 0)$ for $n_2 < n_1$.

Note that when $n_1 = n_2$, then we have

$$(4.2) \quad K_\xi(x_1, n; x_2, n) = \frac{\sin(\phi(x_1 - x_2))}{\pi(x_1 - x_2)}, \quad \phi = \arg(\xi),$$

which justifies the second name of K_ξ which is the *extended sine kernel*.

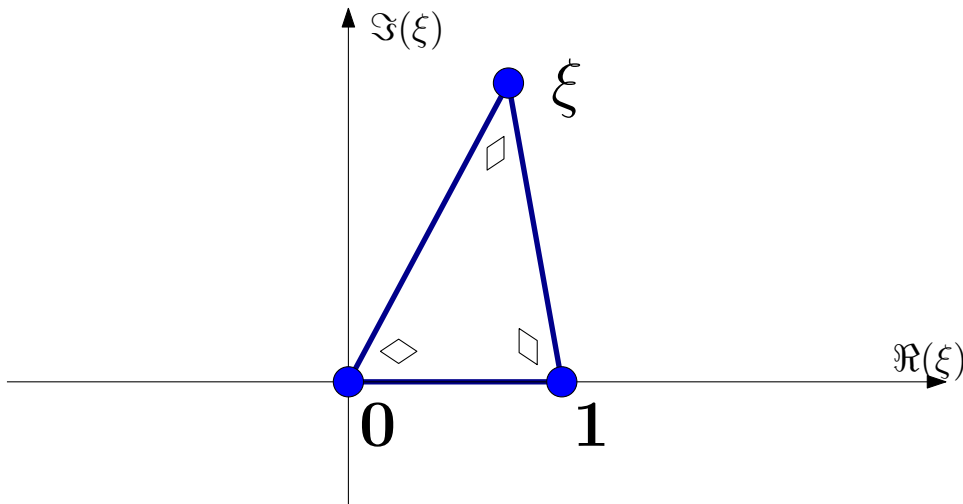


FIGURE 11. Correspondence between complex slope ξ and local proportions of lozenges identifies with angles of a triangle.

Further, we define P_ξ as a probability measure on lozenge tilings of the plane with correlation functions of *horizontal* lozenges given for each $k = 1, 2, \dots$ by:

$$(4.3) \quad P_\xi[\text{there is a horizontal lozenge at } (x_i, n_i), 1 \leq i \leq k] = \det_{i,j=1}^k [K_\xi(x_i, n_i; x_j, n_j)].$$

It is known that P_ξ is a translation invariant ergodic Gibbs measure, cf. [She], [KOS]. We call ξ the *complex slope*. The P_ξ -average proportions p^\square , p^\lozenge , and p^\diamond of three types of lozenges can be reconstructed through the following geometric procedure (see [KOS], [KO]): they are the angles of the triangle on \mathbb{C} with vertices 0, 1 and ξ normalized to sum up to 1, see Figure 11. In particular, $p^\diamond = \frac{1}{\pi} \arg(\xi)$, which matches (4.2) at $x_1 = x_2$. The triplet $(p^\square, p^\lozenge, p^\diamond)$ is the (geometric) slope of P_ξ . [She] shows that P_ξ is a *unique* translation invariant ergodic measure of such slope.

The restriction of P_ξ to horizontal lozenges on a vertical line is described by the kernel (4.2) and has the name *discrete Sine process*.

Theorem 4.1. *For each $N = 1, 2, \dots$, let $\mathbf{t}^N = (t_1^N > t_2^N > \dots > t_N^N)$ be a random N -tuple of integers. Suppose that:*

- *For $\varepsilon > 0$ the random variables $\frac{1}{N} \sum_{i=1}^N \ln^{1+\varepsilon} (1 + |t_i^N|/N)$ are tight as $N \rightarrow \infty$.*
- *The random probability measures $\mu_N = \frac{1}{N} \sum_{i=1}^N \delta_{t_i^N/N}$ converge weakly, in probability to a deterministic measure μ .*

Take a sequence $\mathcal{P}(N)$ of probability measures on trapezoids, such that for each $N = 1, 2, \dots$, the vector \mathbf{t}^N is $\mu_{\mathcal{P}(N)}$ -distributed. Take any point $(\mathbf{x}, \boldsymbol{\eta})$ with $0 < \boldsymbol{\eta} < 1$, such that the complex number $\xi(\mu, \mathbf{x}, \boldsymbol{\eta})$ is well-defined. If $n(N), x(N)$ are two sequences of integers, such that $\lim_{N \rightarrow \infty} n(N)/N = \boldsymbol{\eta}$, $\lim_{N \rightarrow \infty} x(N)/N = \mathbf{x}$, then the point process of $\mathcal{P}(N)$ -distributed lozenges near the point $(x(N), n(N))$ weakly converges as $N \rightarrow \infty$ to $P_{\xi(\mu, \mathbf{x}, \boldsymbol{\eta})}$

Remark 4.2. In more details, the last claim says that if $\rho_k^{(N)}(x_1, n_1; x_2, n_2; \dots; x_k, n_k)$ is the k th correlation function computing the probability that there is a horizontal lozenge at each of the positions (x_i, n_i) , $i = 1, 2, \dots, k$, in the $\mathcal{P}(N)$ -random lozenge tiling, then for each $k = 1, 2, \dots$, and each N -dependent collection of integers $(x_1, n_1; x_2, n_2; \dots; x_k, n_k)$, such that the differences $x_i - x(N)$ and $n_i - n(N)$ do

not depend on N , the limit $\lim_{N \rightarrow \infty} \rho_k^{(N)}(x_1, n_1; x_2, n_2; \dots; x_k, n_k)$ exists and is given by (4.3).

Proof of Theorem 4.1. We fix k and $x_1, n_1; \dots, x_k, n_k$, and aim to compute $\lim_{N \rightarrow \infty} \rho_k^{(N)}(x_1, n_1; x_2, n_2; \dots; x_k, n_k)$. For $y = (y_1 > \dots, y_N)$, let $\rho_k^y(\cdot)$ denote the k th correlation function of horizontal lozenges in tilings corresponding to uniformly random Gelfand–Tsetlin schemes with *fixed* top row y . Then we can write

$$(4.4) \quad \rho_k^{(N)} = \mathbb{E}_{\tau^N} \left[\rho_k^{\tau^N} \right].$$

Theorem 2.1 expresses $\rho_k^y(x_1, n_1; \dots, x_k, n_k)$ as a determinant involving correlation kernel $K(\cdot)$ given by (2.1). The next step is to apply Theorem 2.3 and we need to check that its assumptions are satisfied.

Choose $\delta > 0$ such that δ -neighborhood of $\tau(\mu, \mathbf{x}, \mathbf{n})$ is bounded away from the real axis. The weak convergence of μ_N towards μ and tightness of $\frac{1}{N} \sum_{i=1}^N \ln^{1+\varepsilon}(1 + |\mathbf{t}_i^N|)$ imply that for $G_i(z)$ defined through (cf. (2.2))

$$G_i(z) = \sum_{a=1}^{N-n(N)-n_i} \ln(z - x(N) - x_i + a) - \sum_{r=1}^N \ln(z - \mathbf{t}_r^N), \quad i = 1, \dots, k$$

we have $G_i'(Nz) \rightrightarrows G_i'(z)$ in probability, and therefore the rescaled by N critical points of G_i are in δ -neighborhood of $\tau(\mu, \mathbf{x}, \boldsymbol{\eta})$ with probability tending to 1 as $N \rightarrow \infty$. We conclude that with probability tending to 1 the assumptions of Theorem 2.3 are valid and we can use it to conclude that

$$K(n_i, x_i; n_j, x_j) = \frac{1}{2\pi \mathbf{i}} \int_{\bar{\xi}(N)}^{\xi(N)} w^{x_j - x_i - 1} (1 - w)^{n_j - n_i} + o(1),$$

where $o(1)$ is a remainder which tends to 0 in probability as $N \rightarrow \infty$, and

$$\xi(N) = \frac{\tau_i/N - x_i/N - x(N)/N}{\tau_i/N - x_i/N - x(N)/N + 1 - n_i/N - n(N)/N}$$

with τ_i being the critical point of G_i in the upper half-plane.

As $N \rightarrow \infty$, $\xi(N)$ converges in probability to

$$\xi = \frac{\tau(\mu, \mathbf{x}, \boldsymbol{\eta}) - \mathbf{x}}{\tau(\mu, \mathbf{x}, \boldsymbol{\eta}) - \mathbf{x} + 1 - \boldsymbol{\eta}}.$$

Since the random variable under expectation in (4.4) is between 0 and 1, the convergence in probability implies the convergence of expectations and therefore

$$(4.5) \quad \lim_{N \rightarrow \infty} \rho_k^{(N)}(n_1, x_1; \dots, n_k, x_k) = \det_{i,j=1}^k \left[\frac{1}{2\pi \mathbf{i}} \int_{\bar{\xi}(\mu, \mathbf{x}, \boldsymbol{\eta})}^{\xi(\mu, \mathbf{x}, \boldsymbol{\eta})} w^{x_j - x_i - 1} (1 - w)^{n_j - n_i} \right]. \quad \square$$

The next step is to link the complex slope ξ of Theorem 4.1 to the limit shape for the height function, as discussed in Section 3.

Theorem 4.3. *For each $N = 1, 2, \dots$, let $\mathbf{t}^N = (\mathbf{t}_1^N > \mathbf{t}_2^N > \dots > \mathbf{t}_N^N)$ be a random N -tuple of integers. Suppose that:*

- *There exists $C > 0$ such that $|\mathbf{t}_i^N| < CN$ almost surely for all $1 \leq i \leq N$.*
- *The random probability measures $\mu_N = \frac{1}{N} \sum_{i=1}^N \delta_{\mathbf{t}_i^N/N}$ converge weakly, in probability to a deterministic measure μ .*

Take a sequence $\mathcal{P}(N)$ of probability measures on trapezoids, such that for each $N = 1, 2, \dots$, the vector \mathbf{t}^N is $\mu_{\mathcal{P}(N)}$ -distributed. Then the rescaled height function (cf. Theorem 3.1) converges as $N \rightarrow \infty$ uniformly, in probability to a non-random limit shape $H_\mu(\mathbf{x}, \boldsymbol{\eta})$, $x \in \mathbb{R}$, $0 \leq \boldsymbol{\eta} \leq \mathbf{1}$, in the coordinate system of Figure 5; this limit shape is encoded by three proportions of lozenges $(p^\square(\mathbf{x}, \boldsymbol{\eta}), p^\triangleleft(\mathbf{x}, \boldsymbol{\eta}), p^\triangleright(\mathbf{x}, \boldsymbol{\eta}))$.

Take any point $(\mathbf{x}, \boldsymbol{\eta})$ with $0 < \boldsymbol{\eta} < 1$, such that the proportions of lozenges are continuous and non-zero at this point. Then the complex number $\xi(\mu, \mathbf{x}, \boldsymbol{\eta})$ is well-defined, and moreover $(p^\square(\mathbf{x}, \boldsymbol{\eta}), p^\triangleleft(\mathbf{x}, \boldsymbol{\eta}), p^\triangleright(\mathbf{x}, \boldsymbol{\eta}))$ are precisely the normalized angles of the triangle $0, 1, \xi(\mu, \mathbf{x}, \boldsymbol{\eta})$. And vice-versa, if the complex number $\xi(\mu, \mathbf{x}, \boldsymbol{\eta})$ is well-defined, then the proportions of lozenges at $(\mathbf{x}, \boldsymbol{\eta})$ are continuous and given by the angles of the $0, 1, \xi(\mu, \mathbf{x}, \boldsymbol{\eta})$ triangle.

Remark 4.4. The assumption $|\mathbf{t}_i^N| < CN$ of Theorem 4.3 is much more restrictive than the tightness assumption in Theorem 4.1. Probably, $|\mathbf{t}_i^N| < CN$ can be weakened, but we will not go into this direction.

Proof of Theorem 4.3. The first part of the theorem, i.e. the convergence of the height function to a non-random limit shape $H_\mu(\mathbf{x}, \boldsymbol{\eta})$ is a direct corollary of Theorem 3.1, as the weak convergence of measures μ_N implies the convergence of the height functions (which are their distribution functions) along the right boundary.

For the second part, we need an explicit characterization of $H_\mu(\mathbf{x}, \boldsymbol{\eta})$ obtained in [BuG1] and then further refined in [BuK].

Given a probability measure μ of bounded by 1 density and compact support, define its exponential Stieltjes transform through

$$E_\mu(z) = \exp\left(\int_{\mathbb{R}} \frac{1}{z-x} \mu(dx)\right).$$

$E_\mu(z)$ is an analytic function outside the support of μ . Set

$$(4.6) \quad R_\mu(z) = E_\mu^{(-1)}(z) - \frac{z}{z-1},$$

where $E_\mu^{(-1)}(v)$ is the functional inverse of E_μ , and z is taken to be close to 1 in (4.6) in order for this inverse to be uniquely defined. $R_\mu(z)$ is a close relative of the Voiculescu R -transform of [V], but is slightly different, see [BuG1] for the details.

For $\boldsymbol{\eta} \in (0, 1]$, let $\mu[\boldsymbol{\eta}]$ be a measure on \mathbb{R} with density at a point x equal to $p^\triangleright(\boldsymbol{\eta}\mathbf{x} - \boldsymbol{\eta}, \boldsymbol{\eta})$. Note that $\mu[\boldsymbol{\eta}]$ is a probability measure due to combinatorial constraint on the number of horizontal lozenges on a vertical line. Then the results of [BuG1, Section 3.2]⁴ yield that

$$(4.7) \quad R_{\mu[\boldsymbol{\eta}]}(v) = \frac{1}{\boldsymbol{\eta}} R_{\mu[1]}(v).$$

Let us rewrite the equation (4.7) in a different equivalent form. Let $H(z)$ denote the function $E_{\mu[1]}^{(-1)}$, then plugging $v = E_{\mu[\boldsymbol{\eta}]}(z)$ into (4.7) we get

$$(4.8) \quad \boldsymbol{\eta}z = H(E_{\mu[\boldsymbol{\eta}]}(z)) - \frac{E_{\mu[\boldsymbol{\eta}]}(z)}{E_{\mu[\boldsymbol{\eta}]}(z) - 1} (1 - \boldsymbol{\eta}).$$

⁴There is a technical condition in [BuG1], originating from [GPa] that the distribution function of μ is piecewise-continuous. However, one easily sees that this condition is not important for the proofs. Another way to remove this condition is to use the known continuity of dependence of the limit shape on boundary conditions, see [CEP, Proposition 20] for the corresponding statement and proof for the domino tilings; the proof for lozenge tilings is the same.

We also have

$$(4.9) \quad E_{\mu[1]}(H(E_{\mu[\eta]}(z))) = E_{\mu[\eta]}(z)$$

Express $H(E_{\mu[\eta]}(z))$ from (4.8) and plug it into (4.9) to get

$$(4.10) \quad E_{\mu(1)} \left(\eta z + \frac{E_{\mu[\eta]}(z)}{E_{\mu[\eta]}(z) - 1} (1 - \eta) \right) = E_{\mu[\eta]}(z).$$

Further, let

$$w = \eta z + \frac{E_{\mu[\eta]}(z)}{E_{\mu[\eta]}(z) - 1} (1 - \eta),$$

i.e.

$$\frac{\eta z - w}{\eta z - w + 1 - \eta} = E_{\mu[\eta]}(z),$$

then (4.10) turns into

$$(4.11) \quad E_{\mu[1]}(w) = \frac{\eta z - w}{\eta z - w + 1 - \eta},$$

Now if we set $\eta z - \eta = \mathbf{x}$ and $w = u + 1$, then (4.11) is precisely the equation $G'_{\mu, \mathbf{x}, \eta}(u) = 0$.

Therefore, if the latter has only real roots, then u is necessarily real, which implies that

$$(4.12) \quad \lim_{v \rightarrow \mathbf{x}/\eta + 1} E_{\mu[\eta]}(v)$$

is also real. But since the density of $\mu[\eta]$ is always between 0 and 1, this is possible only when this density at $\mathbf{x}/\eta + 1$ (which is $p^\diamond(\mathbf{x}, \eta)$ by the definition) is either 0 or 1.

Therefore, if at a point (\mathbf{x}, η) the proportions of lozenges are non-zero, then $\xi(\mu, \mathbf{x}, \eta)$ is a well-defined complex number.

It remains to prove that if $\xi(\mu, \mathbf{x}, \eta)$ is well-defined, then $(p^\square(\mathbf{x}, \eta), p^\triangleleft(\mathbf{x}, \eta), p^\diamond(\mathbf{x}, \eta))$ are (normalized) three angles of the triangle with vertices $0, 1, \xi(\mu, \mathbf{x}, \eta)$.

Note that if $\xi(\mu, \mathbf{x}, \eta)$ is a well-defined non-real number, then Theorem 4.3 implies that the average proportion of horizontal lozenges is bounded away from 0 and 1; this bound is uniform in a neighborhood of \mathbf{x}, η , since $\xi(\mu, \cdot, \cdot)$ continuously depends on its two last arguments near \mathbf{x}, η . Therefore, the density of $\mu[\eta]$ is also bounded away from 0 and 1 in a neighborhood of $\mathbf{x}/\eta + 1$ and hence $\lim_{v \rightarrow \mathbf{x}/\eta + 1} E_{\mu[\eta]}(v)$ is non-real.

Recall that (4.11) upon the change of variables $\eta z - \eta = \mathbf{x}$, $w = u + 1$ is precisely $G'_{\mu, \mathbf{x}, \eta}(u) = 0$. Thus, comparing the expressions of $\xi(\mu, \mathbf{x}, \eta)$ through $u (= \tau(\mu, \mathbf{x}, \eta))$ and of $E_{\mu[\eta]}(z)$ through w , we conclude that

$$(4.13) \quad \lim_{v \rightarrow \mathbf{x}/\eta + 1} E_{\mu[\eta]}(v) = \frac{1}{\xi(\mu, \mathbf{x}, \eta)},$$

where the limit is taken from the *upper* half-plane. On the other hand, the definition of $E_{\mu[\eta]}$ implies

$$(4.14) \quad \lim_{v \rightarrow \mathbf{x}/\eta + 1} \arg(E_{\mu[\eta]}(v)) = - \lim_{\varepsilon \rightarrow 0} \int_{-\infty}^{\infty} \frac{\varepsilon}{\varepsilon^2 + t^2} p^\diamond(\mathbf{x} + t, \eta) dt,$$

where the first limit is taken in the *upper* half-plane. Since $f_\varepsilon(t) = \frac{1}{\pi} \cdot \frac{\varepsilon}{\varepsilon^2 + t^2}$ approaches the delta-function as $\varepsilon \rightarrow 0$ (and using also the continuity of $\xi(\mu, \mathbf{x}, \eta)$ under small

perturbations of \mathbf{x}), we conclude that

$$p^\diamond(\mathbf{x}, \boldsymbol{\eta}) = \frac{1}{\pi} \arg(\xi(\mu, \mathbf{x}, \boldsymbol{\eta})),$$

which is precisely one of the angles of the $0, 1, \xi(\mu, \mathbf{x}, \boldsymbol{\eta})$ triangle. In order to identify another angle, define $\xi(\mu, z, \boldsymbol{\eta})$ for z in the upper half-plane as an analytic continuation of $\xi(\mu, \mathbf{x}, \boldsymbol{\eta})$, satisfying

$$(4.15) \quad \frac{1}{\xi(\mu, z, \boldsymbol{\eta})} = E_{\mu[\boldsymbol{\eta}]} \left(\frac{z}{\boldsymbol{\eta}} + 1 \right).$$

Plugging in (4.15) into (4.10), we get

$$\frac{1}{E_{\mu(1)} \left(\boldsymbol{\eta} + z + \frac{1-\boldsymbol{\eta}}{1-\xi(\mu, z, \boldsymbol{\eta})} \right)} = \xi(\mu, z, \boldsymbol{\eta}).$$

Differentiating the last equation with respect to z and $\boldsymbol{\eta}$, one observes an identity (for all z in the upper half-plane)

$$\frac{\xi(\mu, z, \boldsymbol{\eta}) - 1}{\xi(\mu, z, \boldsymbol{\eta})} \cdot \frac{\partial}{\partial \boldsymbol{\eta}} \xi(\mu, z, \boldsymbol{\eta}) = \frac{\partial}{\partial z} \xi(\mu, z, \boldsymbol{\eta}),$$

which is (a version of) the complex inviscid Burgers' equation, cf. [KO].

Since the proportions of lozenges are identified with derivatives of the limiting height function, we can further write (here L is an arbitrary *very large* positive number)

$$(4.16) \quad \begin{aligned} p^\square(\mathbf{x}, \boldsymbol{\eta}) &= \frac{\partial}{\partial \boldsymbol{\eta}} H_\mu(\mathbf{x}, \boldsymbol{\eta}) = -\frac{\partial}{\partial \boldsymbol{\eta}} \int_{\mathbf{x}}^L (1 - p^\diamond(t, \boldsymbol{\eta})) dt = \frac{\partial}{\partial \boldsymbol{\eta}} \int_{\mathbf{x}}^L p^\diamond(t, \boldsymbol{\eta}) dt \\ &= \lim_{\varepsilon \downarrow 0} \frac{\partial}{\partial \boldsymbol{\eta}} \int_{\mathbf{x}}^L \frac{1}{\pi} \arg(\xi(\mu, t + \mathbf{i}\varepsilon, \boldsymbol{\eta})) dt = \frac{1}{\pi} \lim_{\varepsilon \downarrow 0} \Im \int_{\mathbf{x}}^L \frac{\partial}{\partial \boldsymbol{\eta}} \ln(\xi(\mu, t + \mathbf{i}\varepsilon, \boldsymbol{\eta})) dt \\ &= \frac{1}{\pi} \lim_{\varepsilon \downarrow 0} \Im \int_{\mathbf{x}}^L \frac{\frac{\partial}{\partial \boldsymbol{\eta}} \xi(\mu, t + \mathbf{i}\varepsilon, \boldsymbol{\eta})}{\xi(\mu, t + \mathbf{i}\varepsilon, \boldsymbol{\eta})} dt = \frac{1}{\pi} \lim_{\varepsilon \downarrow 0} \Im \int_{\mathbf{x}}^L \frac{1}{\xi(\mu, t + \mathbf{i}\varepsilon, \boldsymbol{\eta}) - 1} \frac{\partial}{\partial t} \xi(\mu, t + \mathbf{i}\varepsilon, \boldsymbol{\eta}) dt \\ &= \frac{1}{\pi} \lim_{\varepsilon \downarrow 0} \Im \left[\ln(1 - \xi(\mu, L + \mathbf{i}\varepsilon, \boldsymbol{\eta})) - \ln(1 - \xi(\mu, \mathbf{x} + \mathbf{i}\varepsilon, \boldsymbol{\eta})) \right]. \end{aligned}$$

We implicitly use in the last computation that $\xi(\mu, t + \mathbf{i}\varepsilon, \boldsymbol{\eta})$ is non-zero due to (4.15), and that it is not equal to 1, since its argument (computed as the integral in the right-hand side of (4.14)) is strictly between 0 and π .

For large positive L , $\xi(\mu, L\varepsilon, \boldsymbol{\eta})$ is a real number smaller than 1 due to (4.15). Therefore, the imaginary part of the first term in the right-hand side of (4.16) vanishes. We conclude that

$$p^\square(\mathbf{x}, \boldsymbol{\eta}) = -\frac{1}{\pi} \arg(1 - \xi(\mu, \mathbf{x}, \boldsymbol{\eta})),$$

which is precisely the formula for the angle of the $(0, 1, \xi(\mu, \mathbf{x}, \boldsymbol{\eta}))$ triangle adjacent to the right vertex. \square

Theorem 4.5. *Consider a sequence of domains Ω_L , $L = 1, 2, \dots$, which approximate (Ω, h) as in Theorem 3.1. In addition suppose that Ω_L^{trap} is a sequence of trapezoids, such that the symmetric difference $\Omega_L \Delta \Omega_L^{\text{trap}}$ is a union of triangles inside the trapezoid and adjacent to its base, cf. Figure 3. Take a sequence of points $x(L), n(L)$ inside $\Omega_L \cap \Omega_L^{\text{trap}}$, such that $\lim_{L \rightarrow \infty} \frac{1}{L}(x(L), n(L)) = (\mathbf{x}, \boldsymbol{\eta})$. If the proportions of lozenges $(p^\square, p^\square, p^\diamond)$ encoding the limit shape H_Ω of Theorem 3.1 are continuous and non-zero at point $(\mathbf{x}, \boldsymbol{\eta})$, then the point process of lozenges near $x(L), n(L)$ is uniformly random*

lozenge tiling of Ω_L converges as $L \rightarrow \infty$ to a translation invariant ergodic Gibbs measure of geometric slope $(p^\natural(\mathbf{x}, \boldsymbol{\eta}), p^\flat(\mathbf{x}, \boldsymbol{\eta}), p^\diamond(\mathbf{x}, \boldsymbol{\eta}))$

Remark 4.6. The convergence is meant in the same sense as in Remark 4.2.

Proof of Theorem 4.5. The proof is a combination of Theorem 3.1 with Theorems 4.1 and 4.3. More precisely, Theorem 3.1 guarantees that the random probability measures describing the positions of horizontal lozenges along the boundary of Ω_L^{trap} converge as $L \rightarrow \infty$, which allows us to use Theorem 4.1 to deduce the bulk limit theorem. Theorem 4.3 then identifies the complex slope in Theorem 4.1 with the complex slope of the limit shape. Since the complex slopes are in-to-one correspondence with geometric slopes $(p^\natural(\mathbf{x}, \boldsymbol{\eta}), p^\flat(\mathbf{x}, \boldsymbol{\eta}), p^\diamond(\mathbf{x}, \boldsymbol{\eta}))$, the latter are identified as well. \square

REFERENCES

- [BKMM] J. Baik, T. Kriecherbauer, K. T. -R. McLaughlin, P. D. Miller, Discrete Orthogonal Polynomials: Asymptotics and Applications. Annals of Mathematics Studies, Princeton University Press, 2007. arXiv: math.CA/0310278
- [BES] Z. Bao, L. Erdos, K. Schnelli, Local law of addition of random matrices on optimal scale. arXiv:1509.07080
- [Bi] P. Biane, Approximate factorization and concentration for characters of symmetric groups. International Mathematics Research Notices 2001 (2001), no. 4, 179–192
- [BBO] A. Borodin, A. Bufetov, G. Olshanski, Limit shapes for growing extreme characters of $U(\infty)$. Annals of Applied Probability, 25, no. 4 (2015), 2339–2381. arXiv:1311.5697.
- [BF] A. Borodin, P. Ferrari, Anisotropic Growth of Random Surfaces in $2 + 1$ Dimensions. Communications in Mathematical Physics, 325, no. 2, (2014) 603–684. arXiv:0804.3035
- [BG] A. Borodin, V. Gorin, Shuffling algorithm for boxed plane partitions. Advances in Mathematics, 220 (2009), no. 6, 1739–1770. arXiv: 0804.3071.
- [BG2] A. Borodin, V. Gorin, Lectures on Integrable Probability. In: Probability and Statistical Physics in St. Petersburg, Proceedings of Symposia in Pure Mathematics, Vol. 91, 155–214. AMS 2016. arXiv:1212.3351
- [BGG] A. Borodin, V. Gorin, A. Guionnet, Gaussian asymptotics of discrete β -ensembles, to appear in Publications mathématiques de l’IHÉS, arXiv:1505.03760
- [BP] A. Borodin, L. Petrov, Integrable probability: From representation theory to Macdonald processes. Probability Surveys 11 (2014), pp. 1–58, arXiv:1310.8007
- [BEY] P. Bourgade, L. Erdos, H.T. Yau, Fixed energy universality for generalized Wigner matrices, to appear in Communications on Pure and Applied Mathematics. arXiv:1407.5606
- [BuG1] A. Bufetov, V. Gorin, Representations of classical Lie groups and quantized free convolution. *Geometric and Functional Analysis (GAFA)*, 25, no. 3 (2015), 763–814. arXiv:1311.5780
- [BuG2] A. Bufetov, V. Gorin, Fluctuations of particle systems determined by Schur generating functions, arXiv:1604.01110
- [BuK] A. Bufetov, A. Knizel, Asymptotic of random domino tilings of rectangular Aztec diamonds, arXiv:1604.01491
- [CEP] H. Cohn, N. Elkies, J. Propp, Local statistics for random domino tilings of the Aztec diamond. Duke Mathematical Journal, 85, no. 1 (1996), 117–166. arXiv:math/0008243
- [CKP] H. Cohn, R. Kenyon, J. Propp, A variational principle for domino tilings. Journal of American Mathematical Society 14 (2001), no. 2, 297–346. arXiv:math/0008220.
- [CLP] H. Cohn, M. Larsen, J. Propp, The Shape of a Typical Boxed Plane Partition. New York Journal of Mathematics, 4(1998), 137–165. arXiv:math/9801059.
- [D] M. Duits, On global fluctuations for non-colliding processes, arXiv:1510.08248
- [DJM] E. Duse, K. Johansson, A. Metcalfe, The Cusp-Airy Process, arXiv:1510.02057
- [DM] E. Duse, A. Metcalfe, Asymptotic geometry of discrete interlaced patterns: Part I, arXiv:1412.6653
- [G] V. Gorin, Non-intersecting paths and Hahn orthogonal polynomial ensemble. Functional Analysis and its Applications, 42 (2008), no. 3, 180–197. arXiv: 0708.2349.

- [GPa] V. Gorin, G. Panova, Asymptotics of symmetric polynomials with applications to statistical mechanics and representation theory. *Annals of Probability*, 43, no. 6, (2015) 3052–3132. arXiv:1301.0634.
- [GPe] V. Gorin, L. Petrov, Universality of local statistics for noncolliding random walks, arXiv:1608.03243.
- [J] K. Johansson, Universality of the local spacing distribution in certain ensembles of hermitian Wigner matrices. *Communications in Mathematical Physics*, 215, no. 3 (2001), 683–705. arXiv:math-ph/0006020
- [JN] K. Johansson, E. Nordenstam, Eigenvalues of GUE minors. *Electronic Journal of Probability* 11 (2006), paper 50, 1342-1371. arXiv:math/0606760.
- [K1] R. Kenyon, Height Fluctuations in the Honeycomb Dimer Model. *Communications in Mathematical Physics*, 281, no. 3 (2008), 675–709. arXiv: math-ph/0405052
- [K2] R. Kenyon, Lectures on dimers. *Statistical mechanics*, 191–230, IAS/Park City Math. Ser., 16, Amer. Math. Soc., Providence, RI, 2009. arXiv:0910.3129
- [KO] R. Kenyon, A. Okounkov, Limit shapes and Burgers equation. *Acta Mathematica*, 199 (2007), no. 2, 263–302. arXiv:math-ph/0507007.
- [KOS] R. Kenyon, A. Okounkov, and S. Sheffield, Dimers and amoebae. *Annals of Mathematics* 163 (2006), 1019–1056, arXiv:math-ph/0311005.
- [LY] B. Landon, H.-T. Yau, Convergence of local statistics of Dyson Brownian motion, arXiv:1504.03605.
- [Nor] E. Nordenstam, Interlaced particles in tilings and random matrices, University dissertation from Stockholm : KTH, 2009.
- [Nov] J. Novak, Lozenge tilings and Hurwitz numbers. *Journal of Statistical Physics*, 161, no. 2 (2015), 509-517. arXiv:1407.7578
- [O] A. Okounkov, Symmetric functions and random partitions, *Symmetric functions 2001: Surveys of Developments and Perspectives* (S. Fomin, ed.), Kluwer Academic Publishers, 2002. arXiv:math/0309074.
- [OR] A. Okounkov, N. Reshetikhin, Correlation functions of Schur process with application to local geometry of a random 3-dimensional Young diagram. *Journal of American Mathematical Society*, 16 (2003), 581–603. arXiv:math.CO/0107056
- [Pa1] G. Panova, Lozenge tilings with free boundaries. *Letters in Mathematical Physics*, 105, no. 11 (2015), 1551-1586. arXiv:1408.0417
- [Pa2] G. Panova, Centrally symmetric lozenge tilings, in preparation.
- [Pe1] L. Petrov, Asymptotics of Random Lozenge Tilings via Gelfand-Tsetlin Schemes. *Probability Theory and Related Fields*, 160, no. 3 (2014), 429–487. arXiv:1202.3901.
- [Pe2] L. Petrov, Asymptotics of Uniformly Random Lozenge Tilings of Polygons. *Gaussian Free Field*, *Annals of Probability* 43, no. 1 (2015), 1–43. arXiv:1206.5123.
- [Shc] T. Shcherbina, On Universality of Bulk Local Regime of the Deformed Gaussian Unitary Ensemble. *Journal of Mathematical Physics, Analysis, Geometry*, vol. 5, no. 4 (2009), pp. 396–433, arXiv:0804.2116.
- [She] S. Sheffield, Random surfaces. *Asterisque* 2005, no. 304. arXiv:math/0304049
- [V] D. Voiculescu, Addition of certain non-commuting random variables, *Journal of Functional Analysis*, 66 (1986), 323-346.
- [W] H. Weyl, *The Classical Groups: Their Invariants and Representations*. Princeton, University Press, 1939.

(Vadim Gorin) DEPARTMENT OF MATHEMATICS, MASSACHUSETTS INSTITUTE OF TECHNOLOGY, CAMBRIDGE, MA, USA, AND INSTITUTE FOR INFORMATION TRANSMISSION PROBLEMS OF RUSSIAN ACADEMY OF SCIENCES, MOSCOW, RUSSIA. E-MAIL: VADICGOR@GMAIL.COM